The Abdus Salam
International Centre for Theoretical Physics

United Nations
Educational, Scientific and
Cultural Organization

IAEA
International Atomic Energy Agency

2148-27

Fifth ICTP Workshop on the Theory and Use of Regional Climate Models

31 May - 11 June, 2010

Simulated hydroclimatic variability of the greater horn of Africa during the transition between bimodal rainfall regimes

ANYAH Richard Ochieng

University of Connecticut
Department of Natural Resources and the Environment
1376 Storrs Road Unit 4087, Storrs CT 06269-4087
U.S.A.

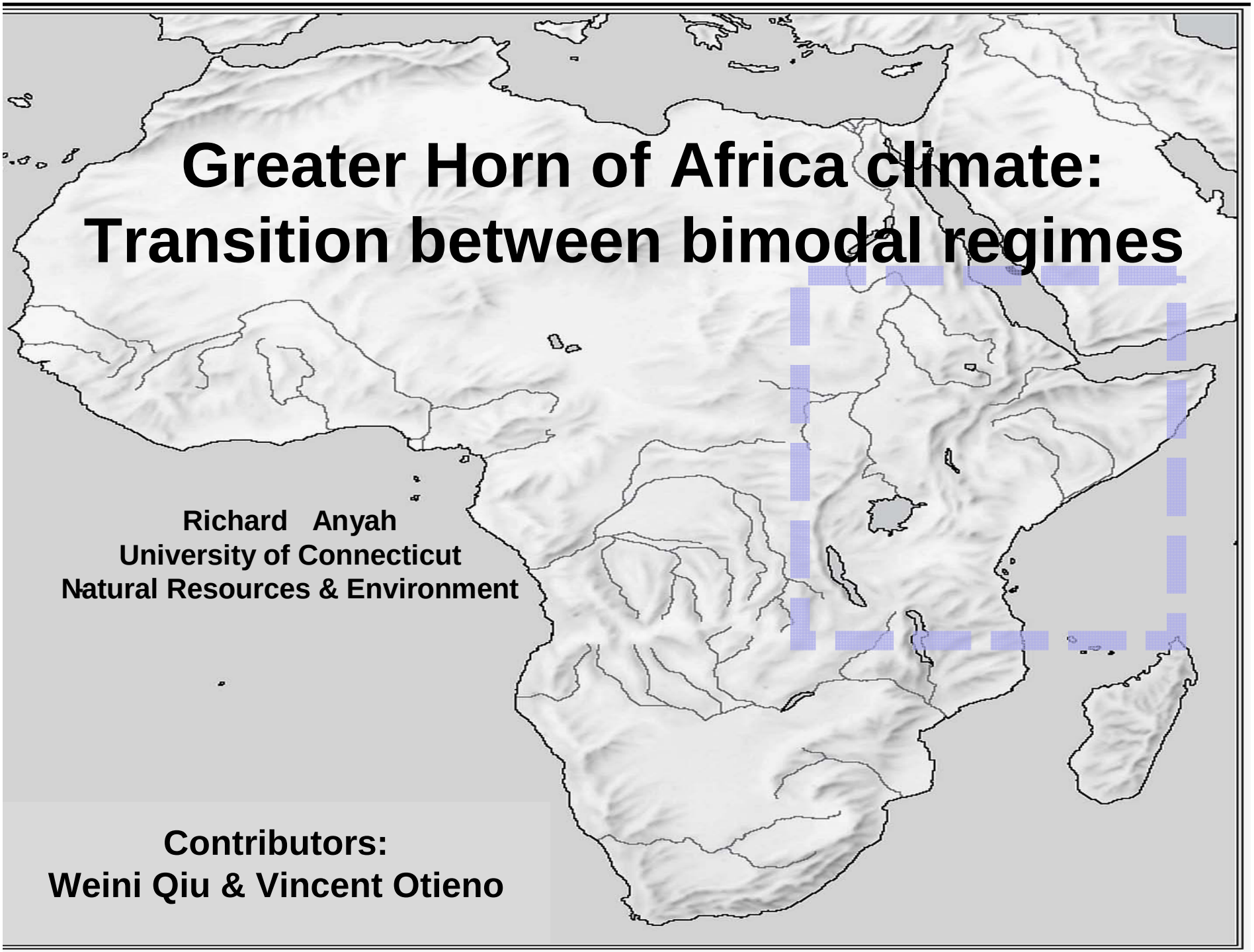

Greater Horn of Africa climate: Transition between bimodal regimes

Richard Anyah
University of Connecticut
Natural Resources & Environment

Contributors:
Weini Qiu & Vincent Otieno

Motivation

- Characterize mechanisms and primary moisture sources and sinks linked to GHA climate (rainfall) variability/anomalies

- Analyze behavior of climate patterns during the transition periods between the two PRIMARY rainfall seasons, especially during anomalous years.

Outline

- Overview of GHA climate
- Why Transition Periods?
- Some Diagnostic Analysis
- RegCM3 Simulations (Present and Future)
- Summary & Conclusions

Greater Horn of Africa (climate drivers)

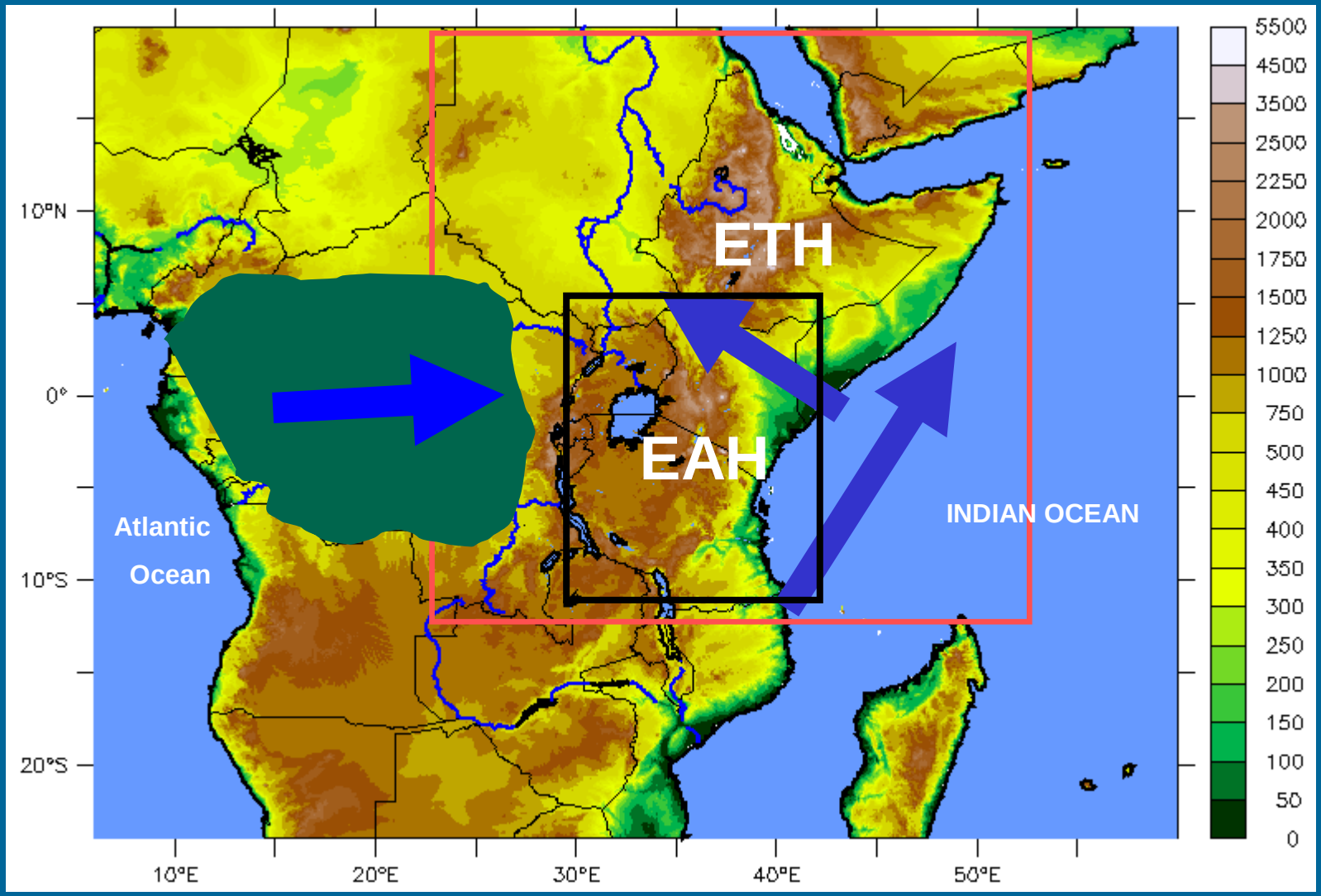

Monthly mean rainfall (mm) over East Africa

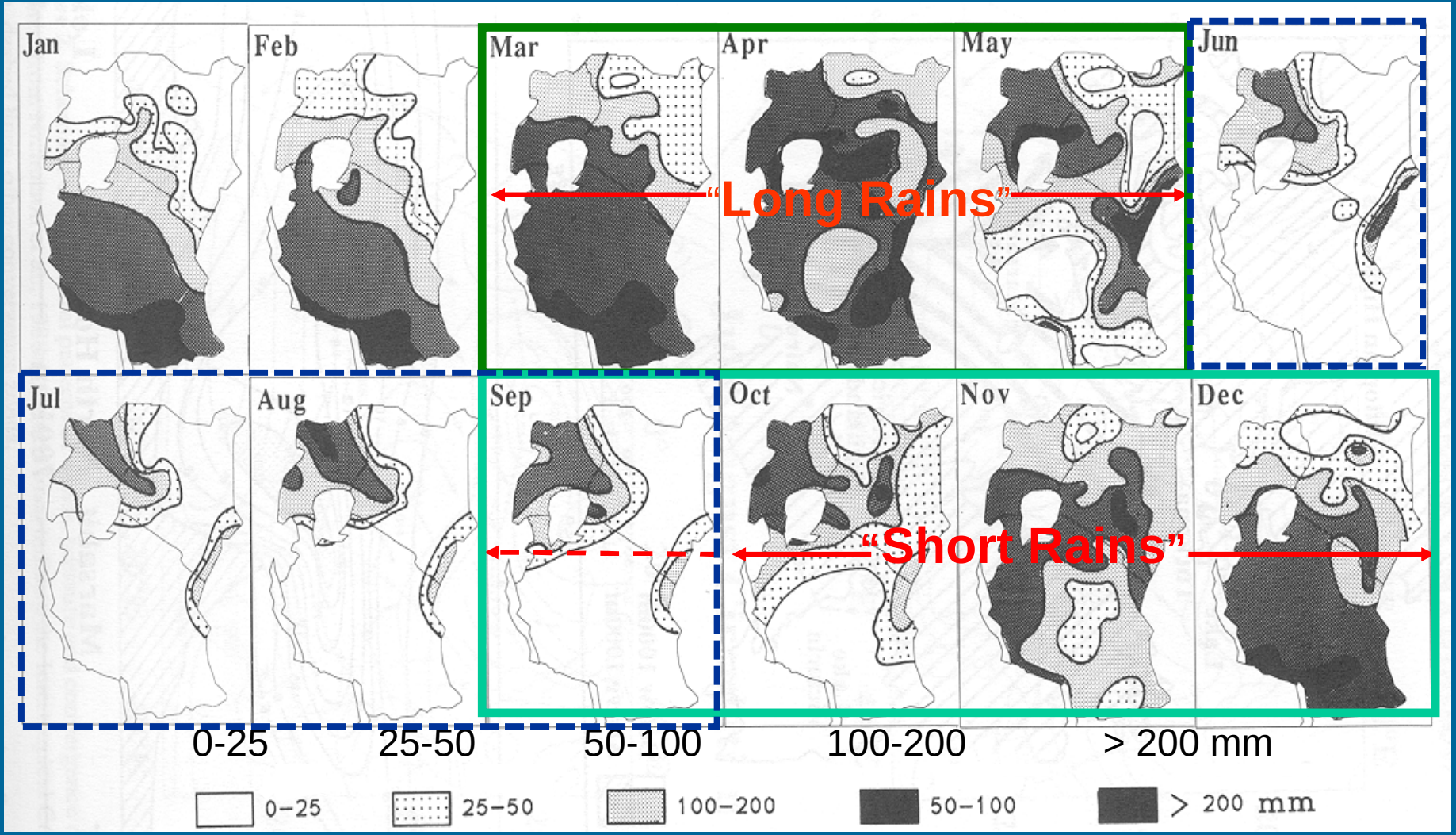

Nyenzi (1992)

Implications of changes in vegetation cover on GHA Climate

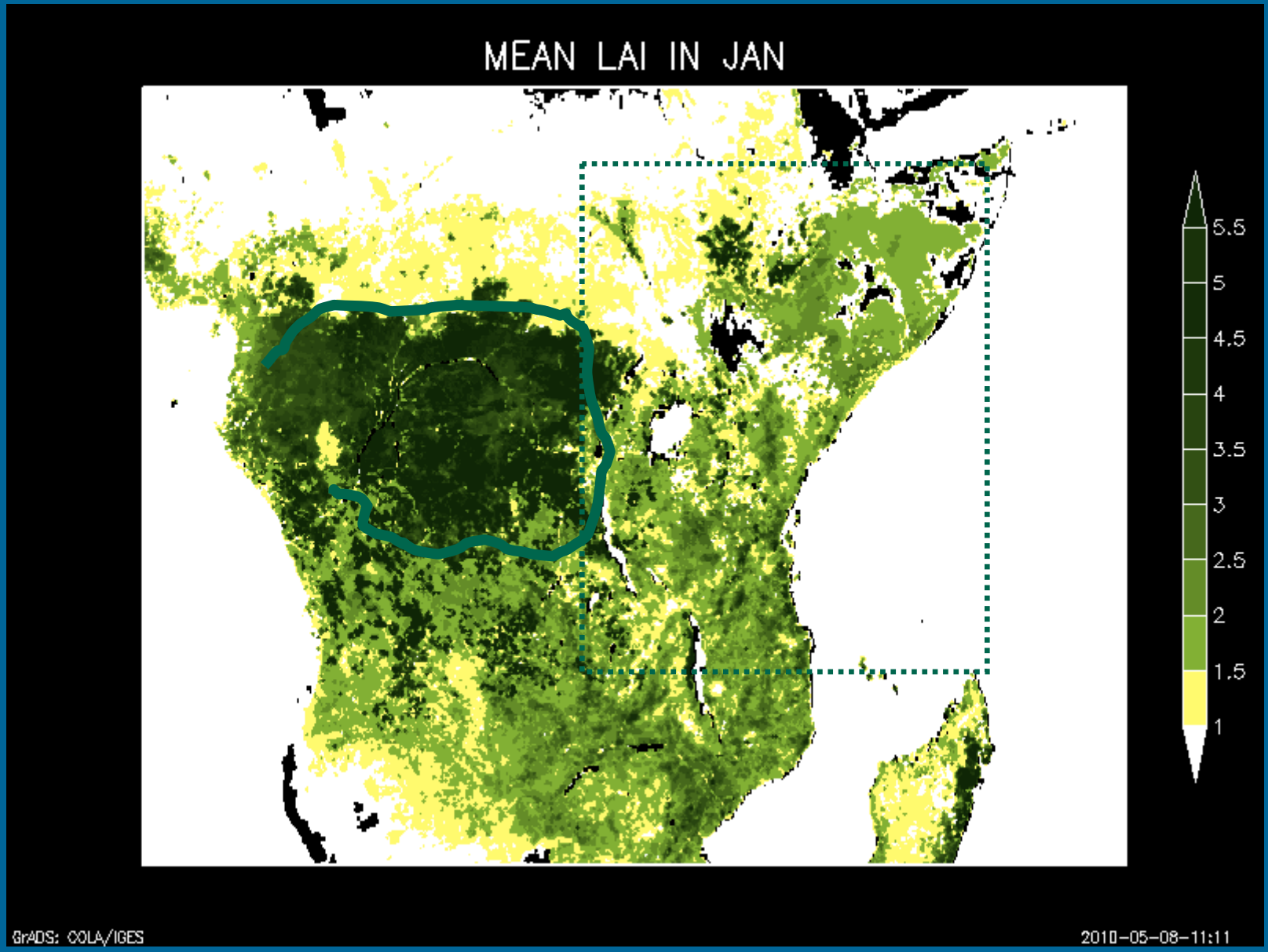

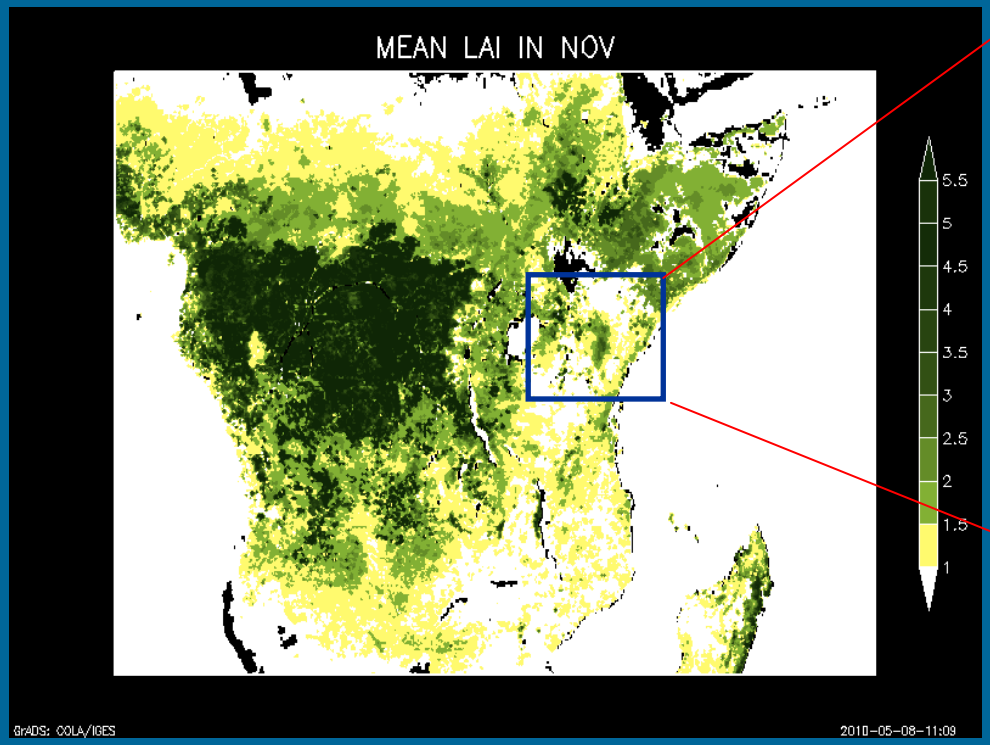

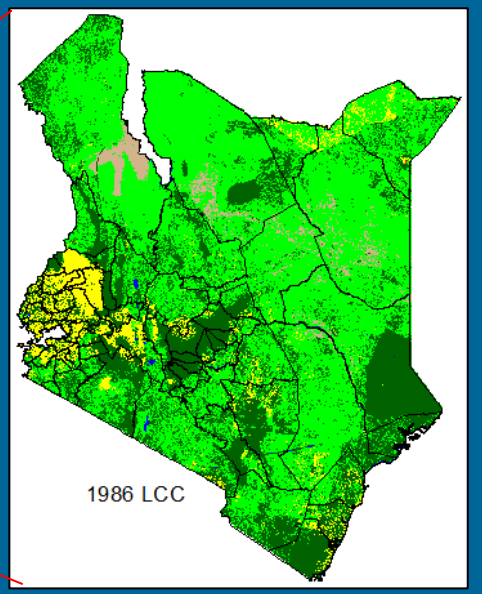

Land Use/Cover Types

- Water Body
- Agricultural fields
- Savannah/Shurb/Grassland
- Dense Vegetation/Forests
- Built up areas
- Barren/Salt mash

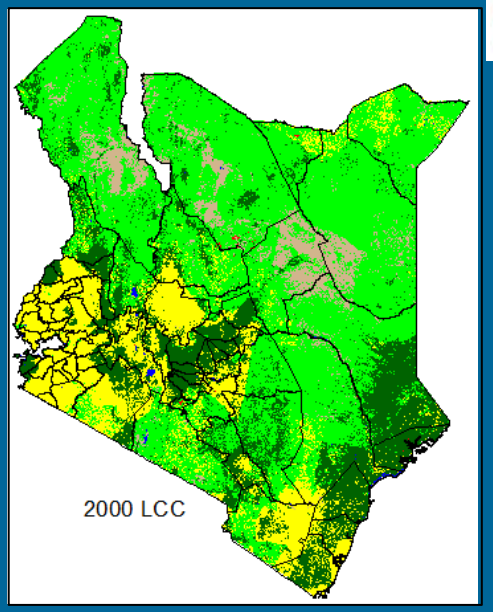

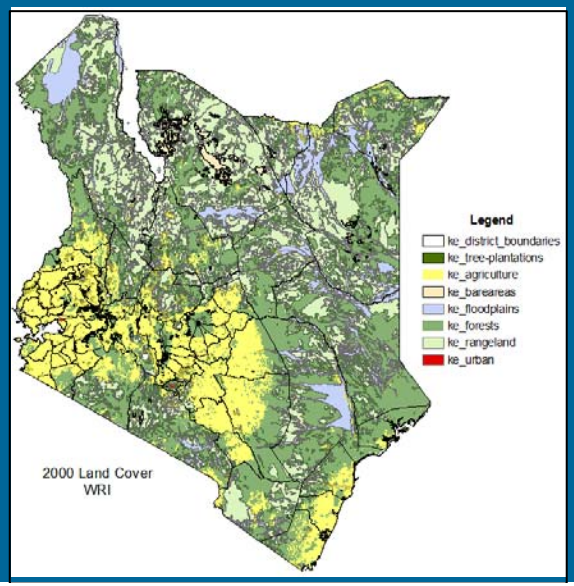

Major river basins in Africa

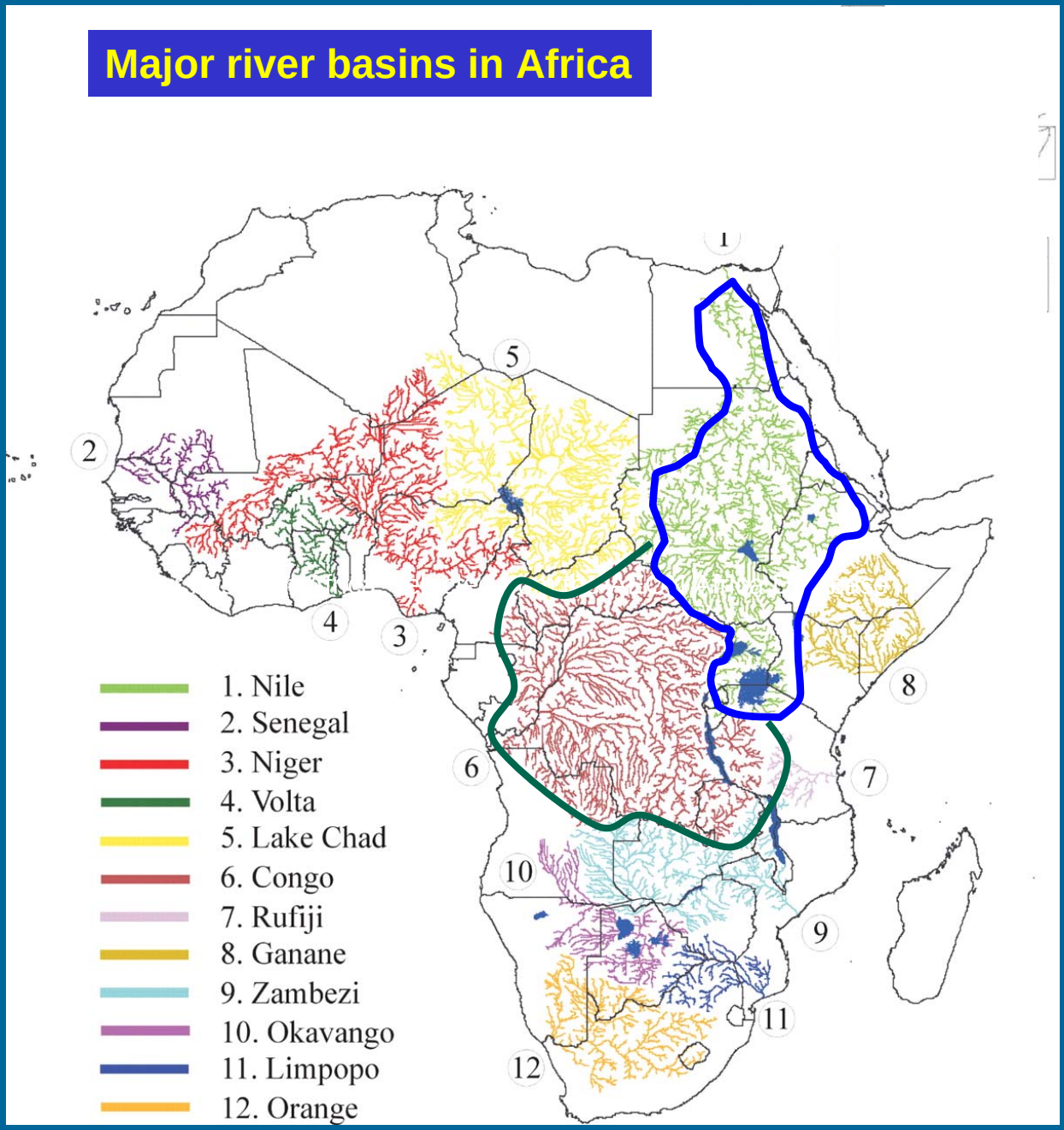

Maarten de Wit and Jacek Stankiewicz (Science, 2006)

SST anomalies and GHA Climate

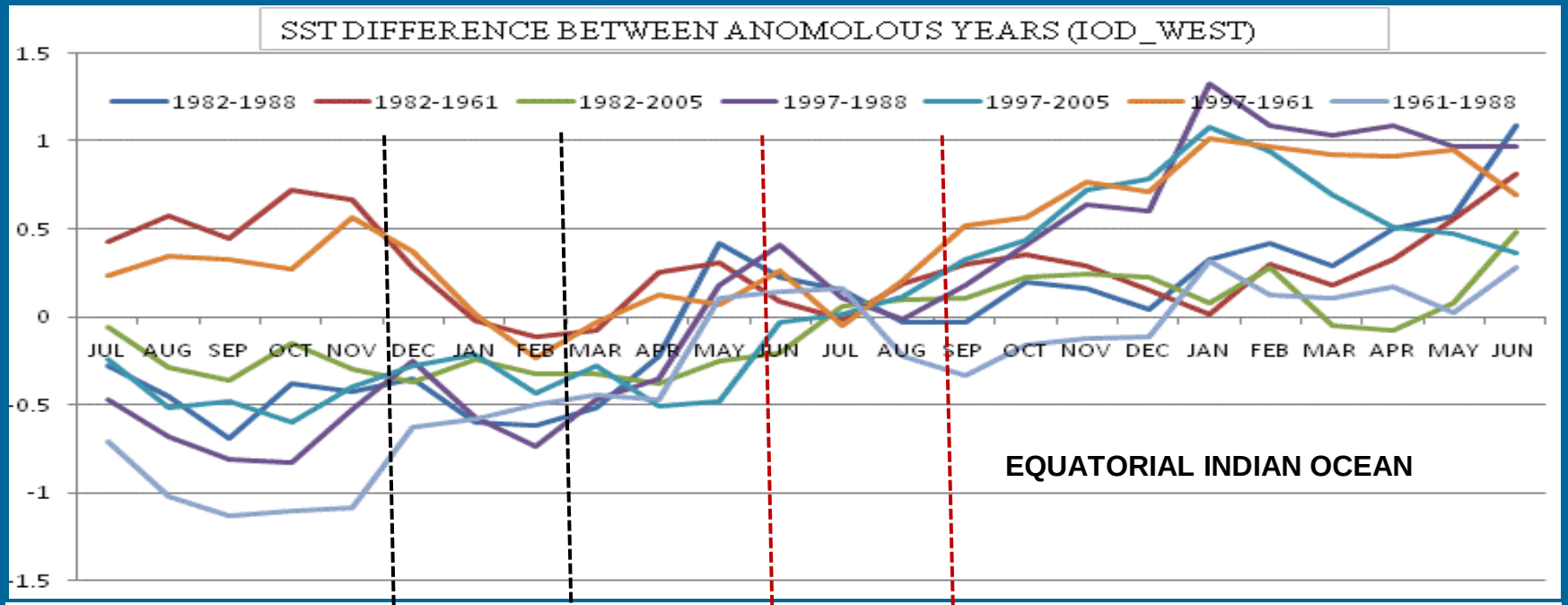

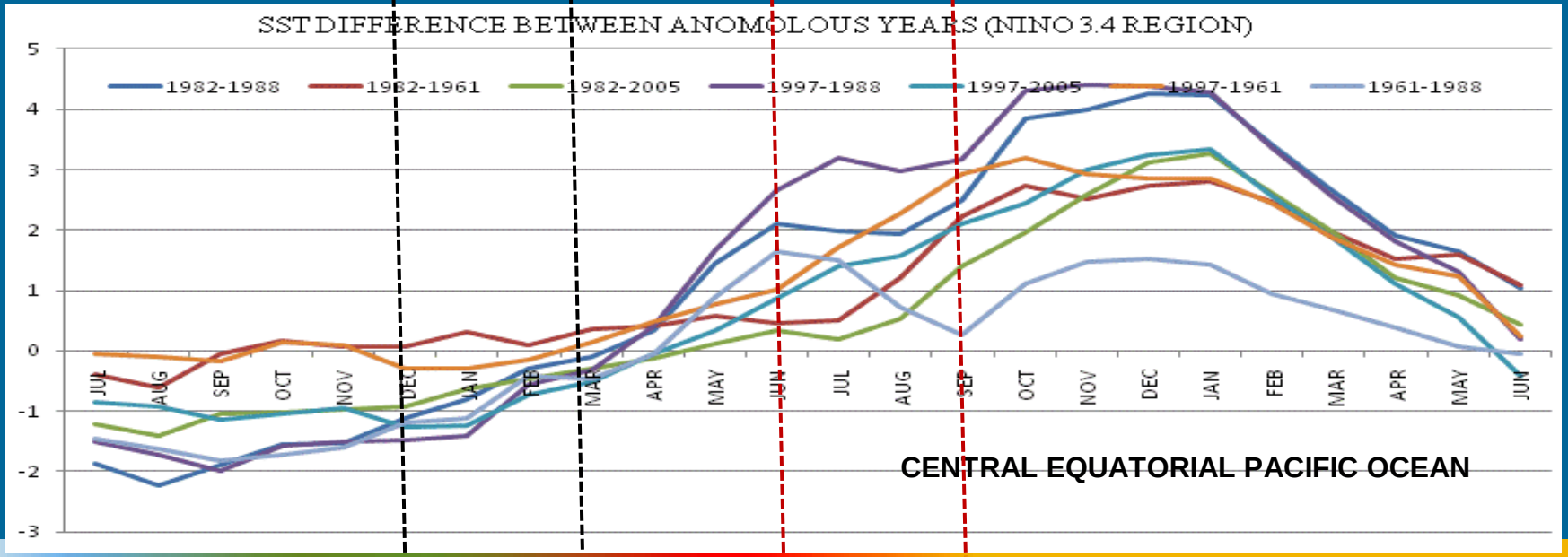

Can RegCM3 preserve spatio-temporal variability associated with large scale forcing ?

ENSO Signal derived from EOF Analysis

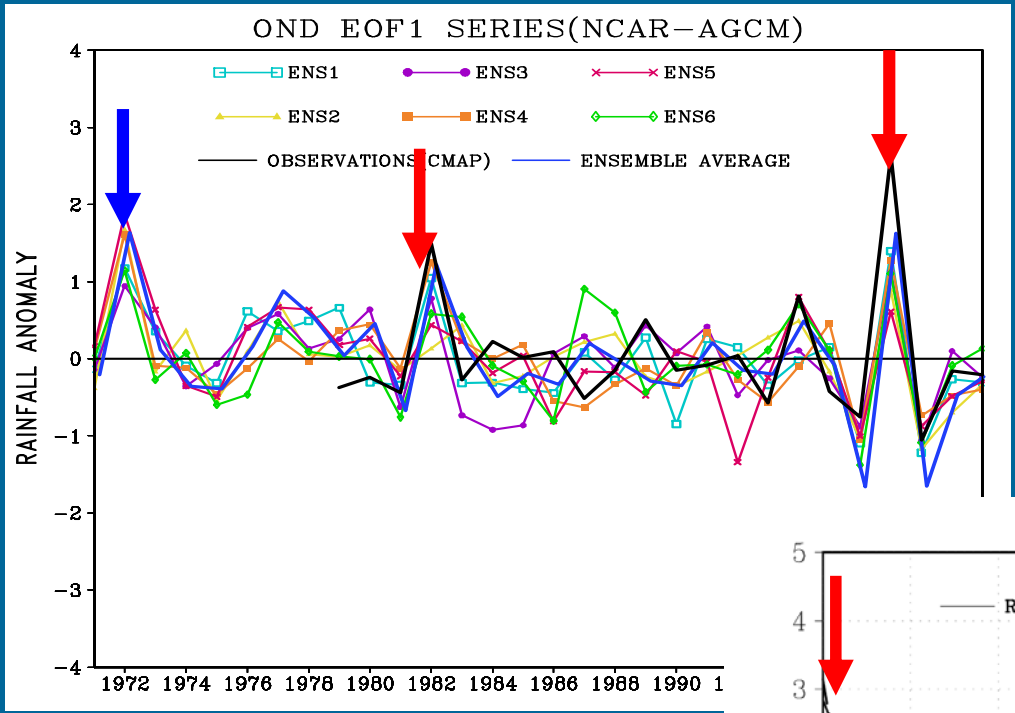

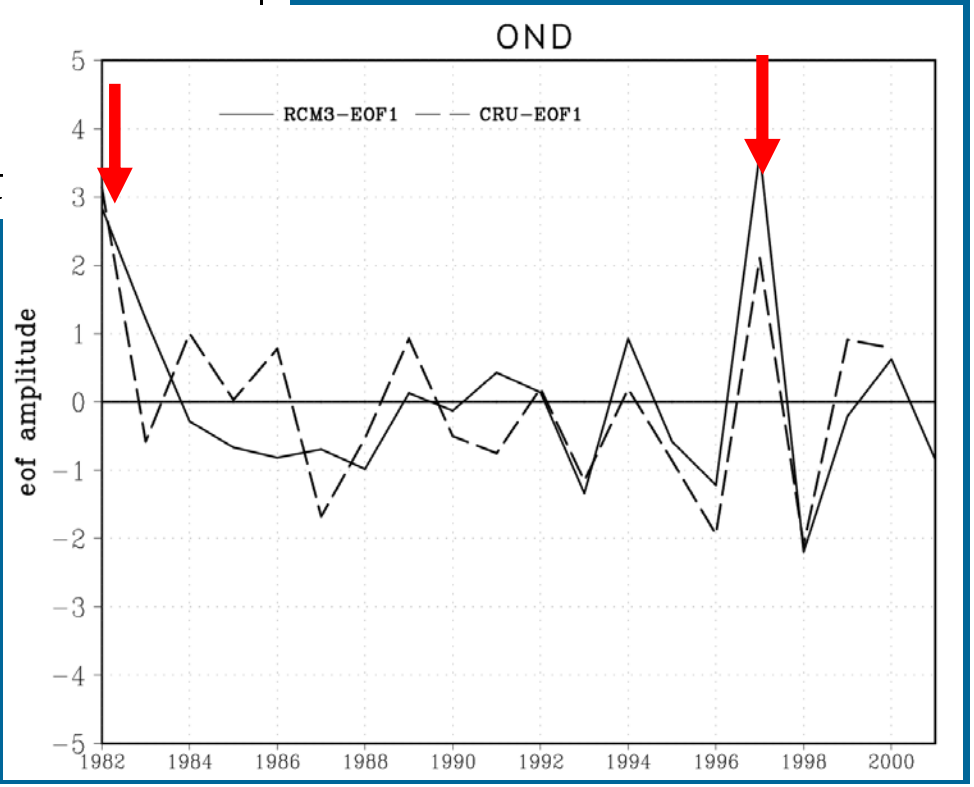

- RegCM3 simulations preserve features of large scale ENSO-related inter-annual variability

Spatial Correlations between rainfall IOD and Nino3.4 indices

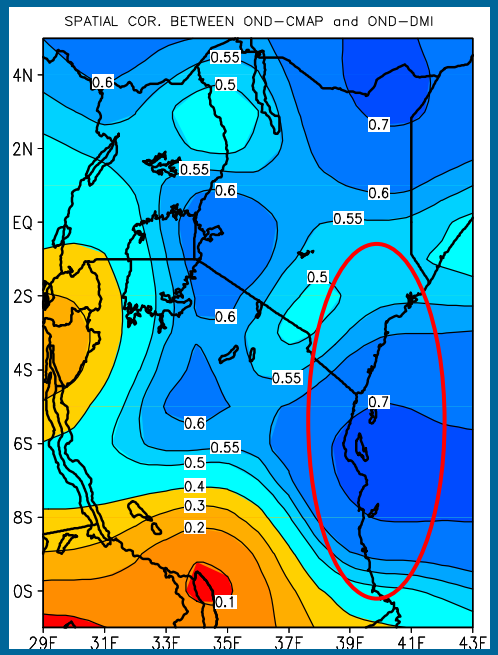

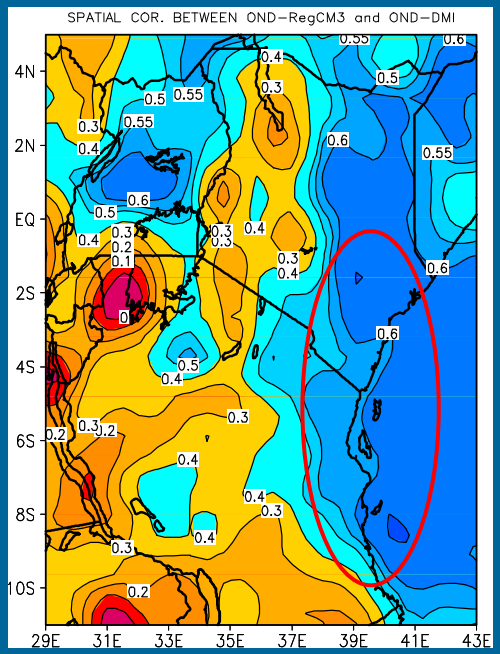

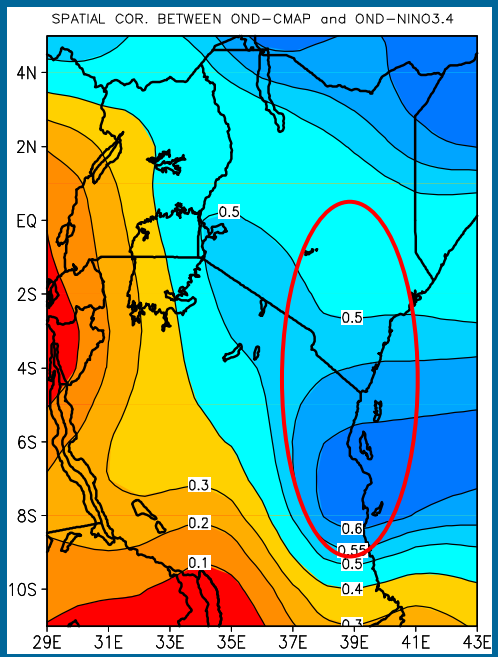

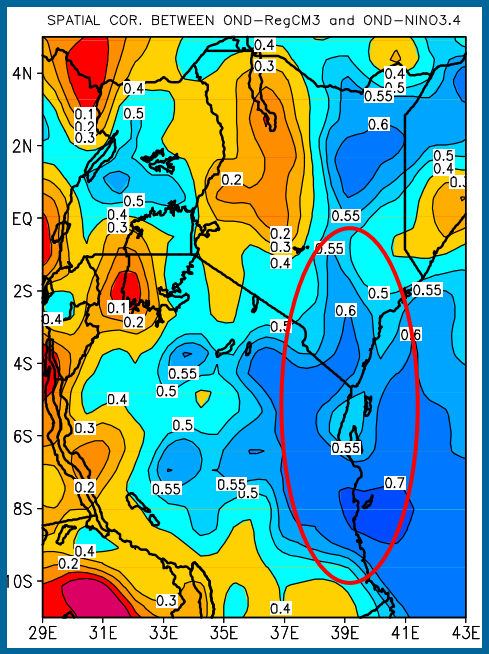

Annual mean rainfall evolution over the Greater Horn of Africa

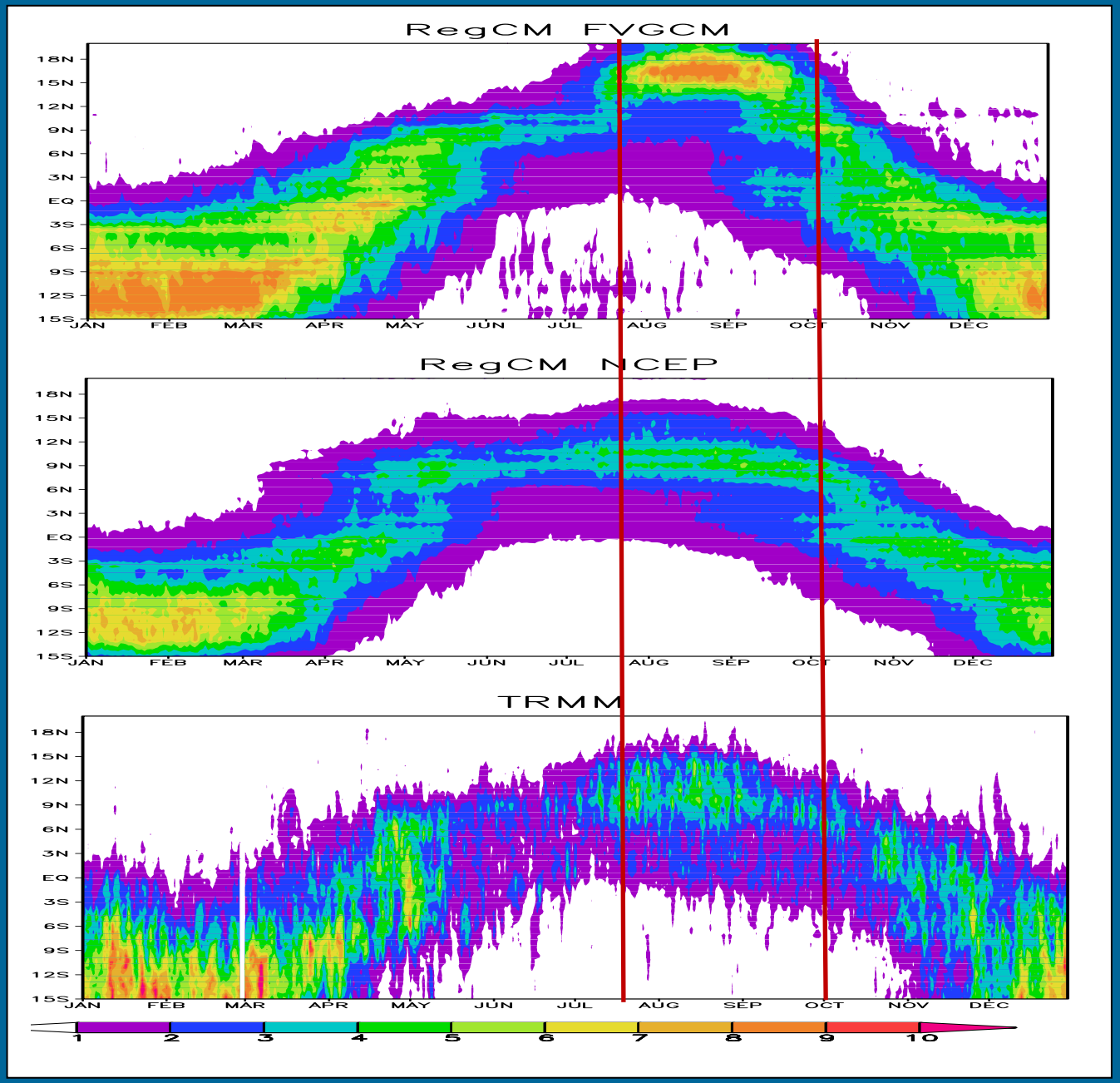

Bowden ,2008

North-south rainfall evolution during short rains RegCM3

CAM2

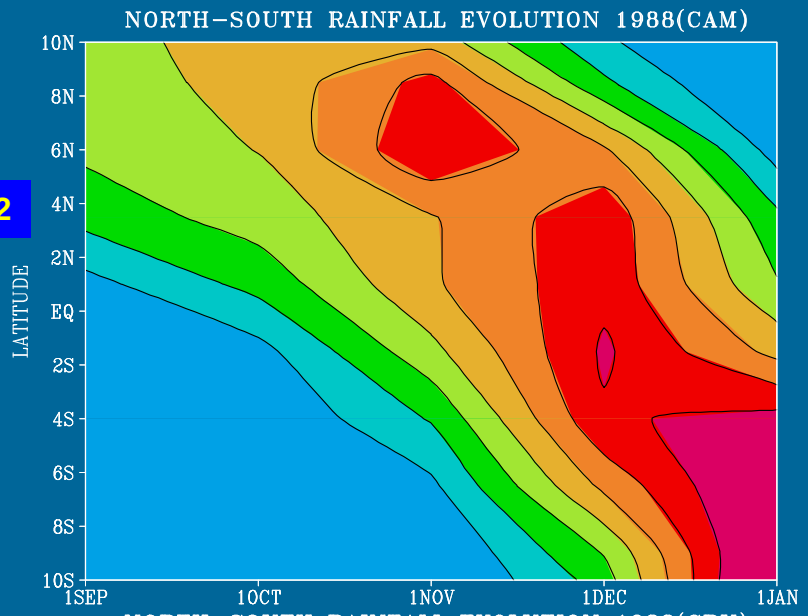

FvGCM

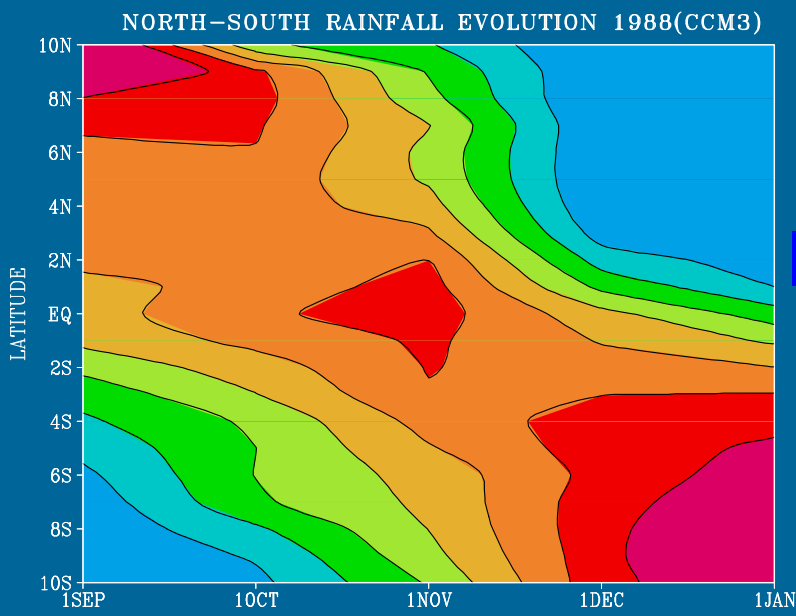

CRU

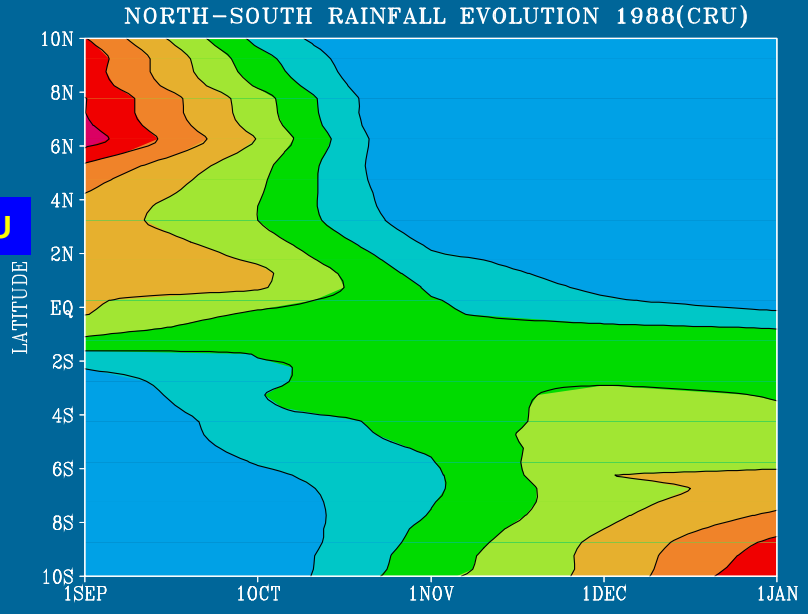

RegCM3

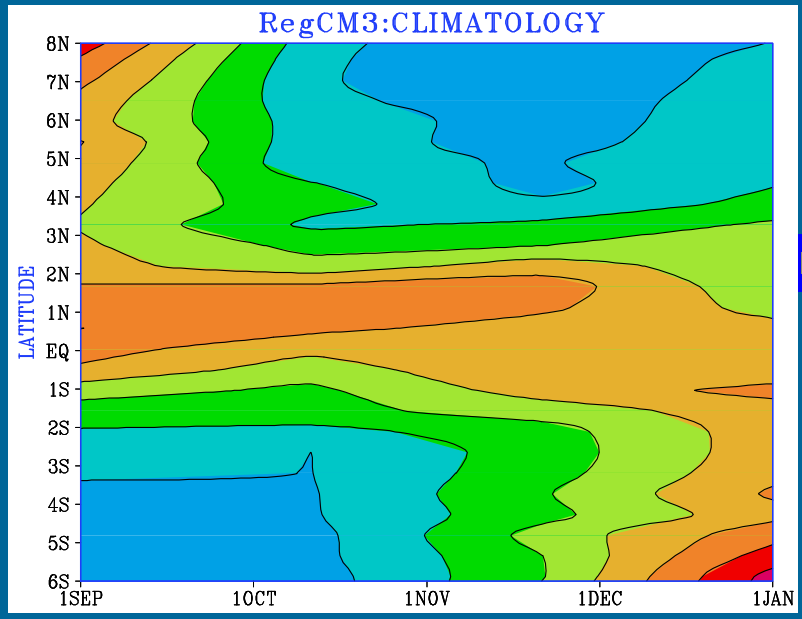

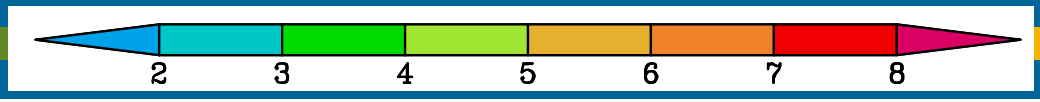

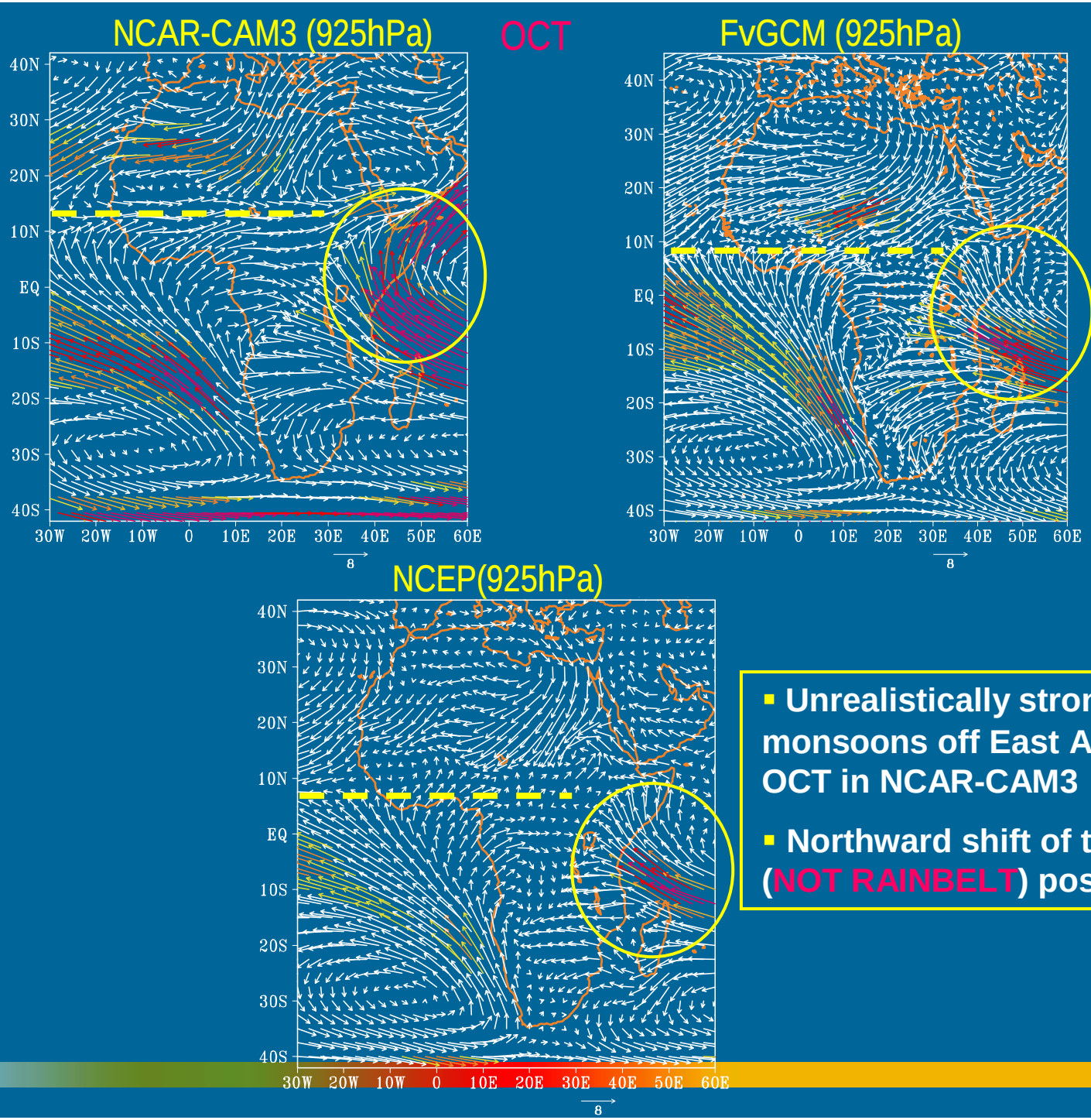
NCAR-CAM3 (925hPa)
OCT
FvGCM (925hPa)
NCEP(925hPa)
40N
30N
20N
10N
EQ
10S
20S
30S
40S
30W 20W 10W 0 10E 20E 30E 40E 50E 60E
8
▪ Unrealistically strong SE/SW monsoons off East Africa coast in OCT in NCAR-CAM3
▪ Northward shift of the ITCZ (NOT RAINBELT) position in GCM

RegCM3 Rainfall Climatology (1981-2000)

RegCM3

CRU

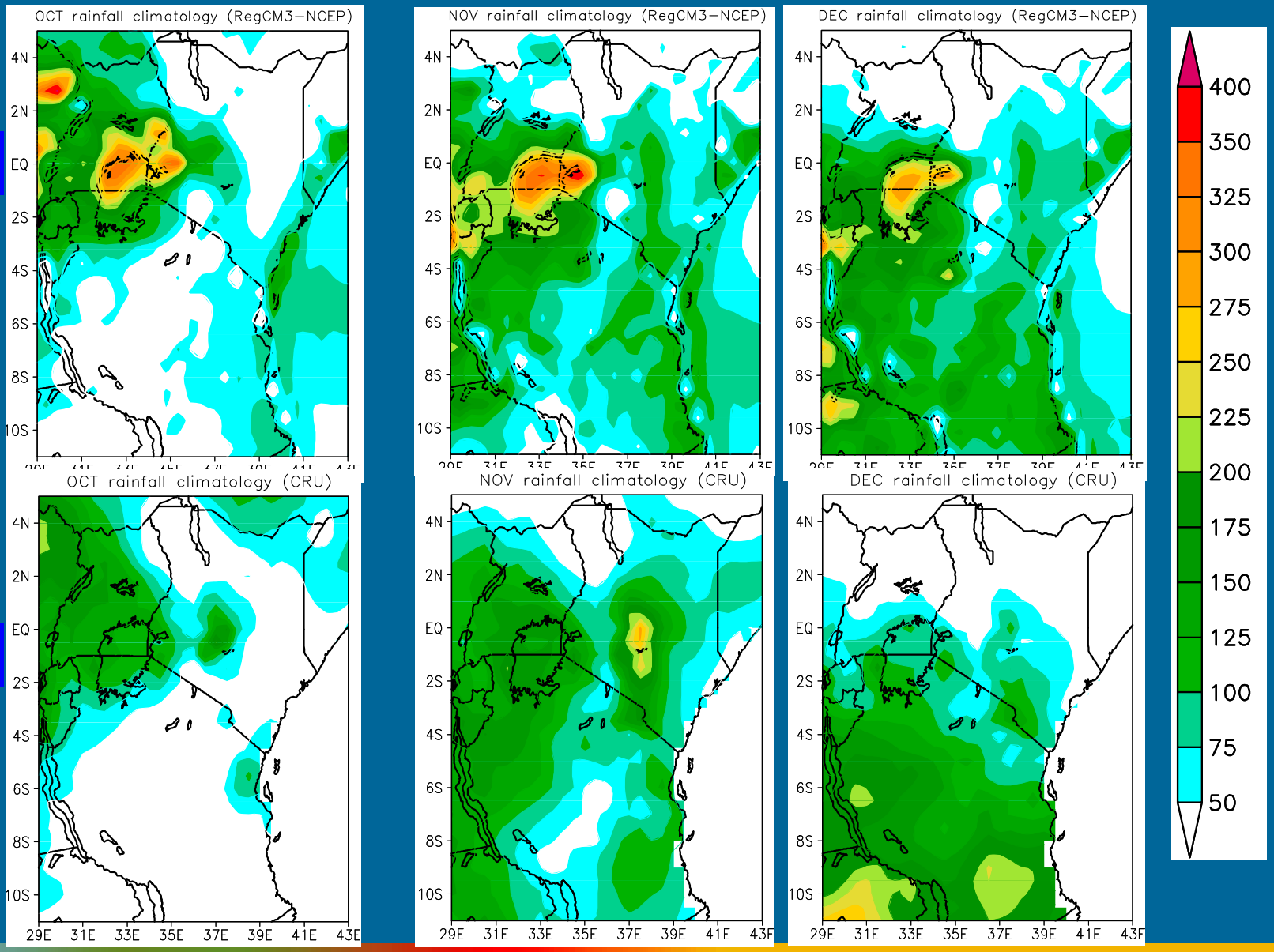

Incorporating role large inland Lakes

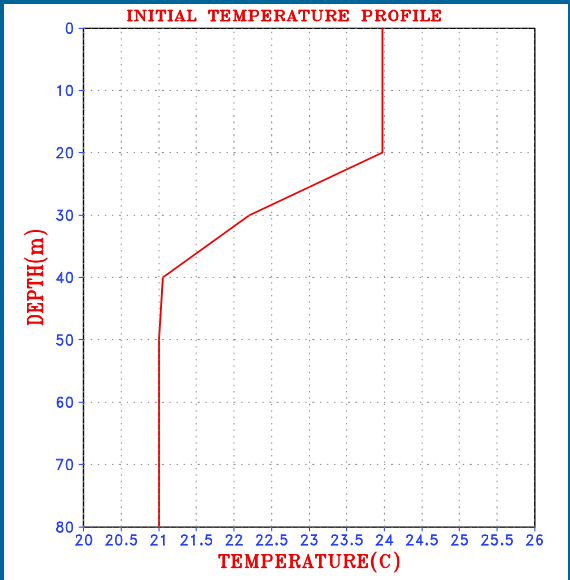

Initialization of Lake model:

- Lake bathymetry (lake points [x,y,z(d)]
- Define number of layers over entire depth
- 9 uniform 5m layers for L. Victoria (shallow)
- Read in LSTs (or initialize with homogeneous LST distribution

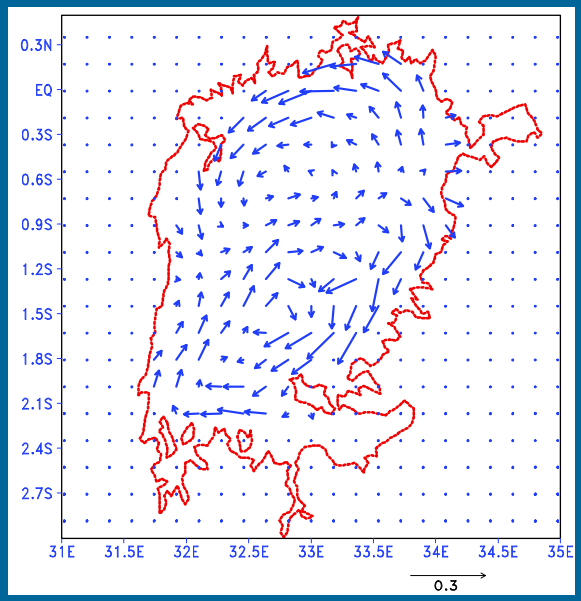

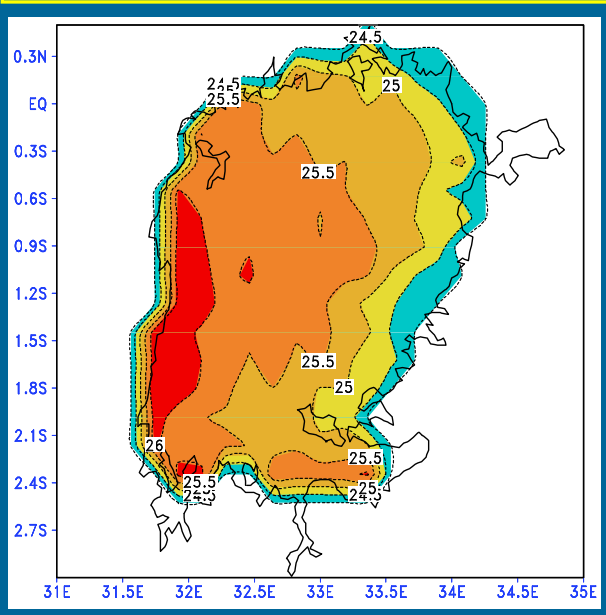

Song et al., 2004;
Anyah et al.,2006,2009

- Western coastline, which is relatively shallower is warmer compared to rest of lake

Simulated vs Observed Rainfall (mm): Transition months

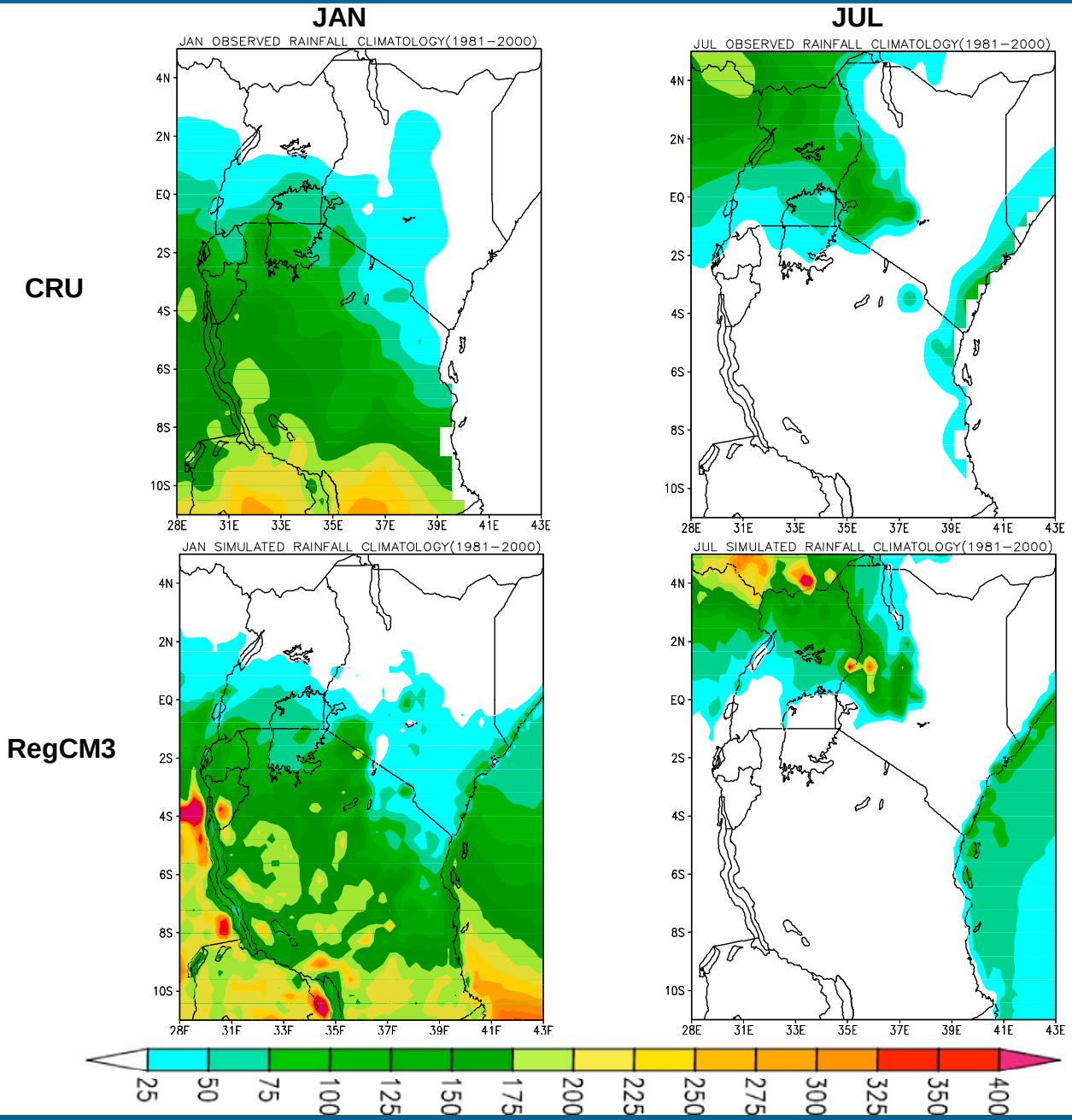

RegCM3 simulated rainfall variability over different homogeneous climate zones

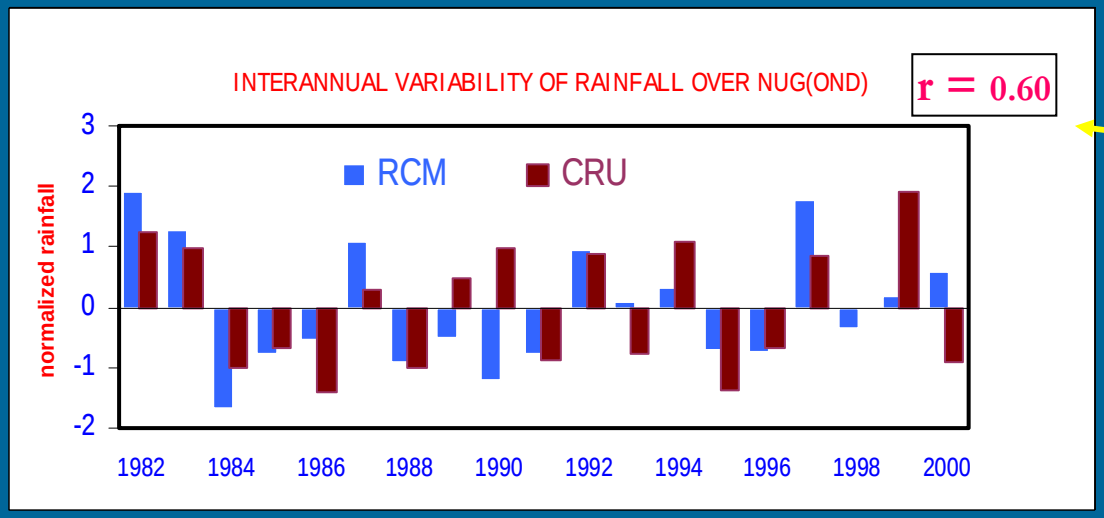

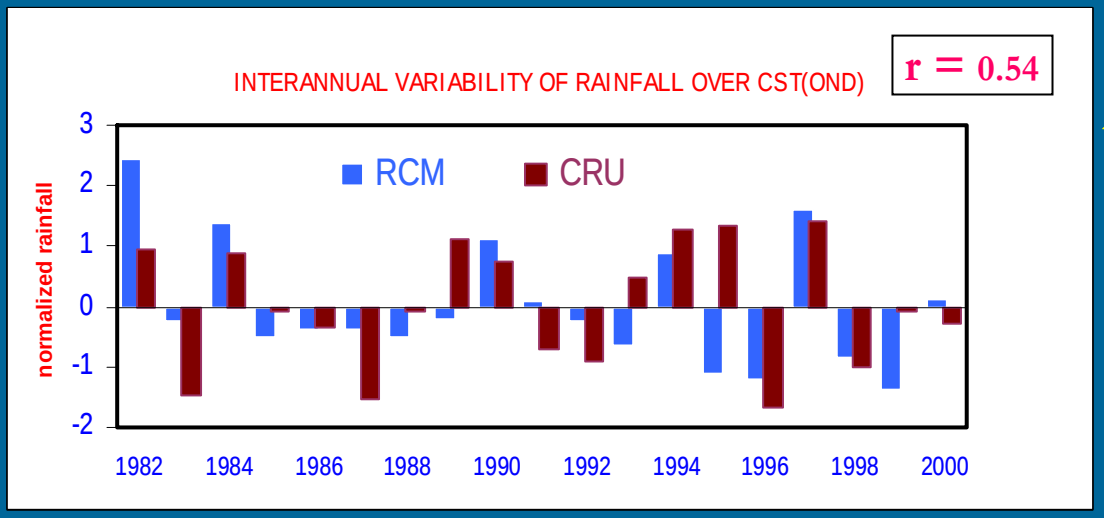

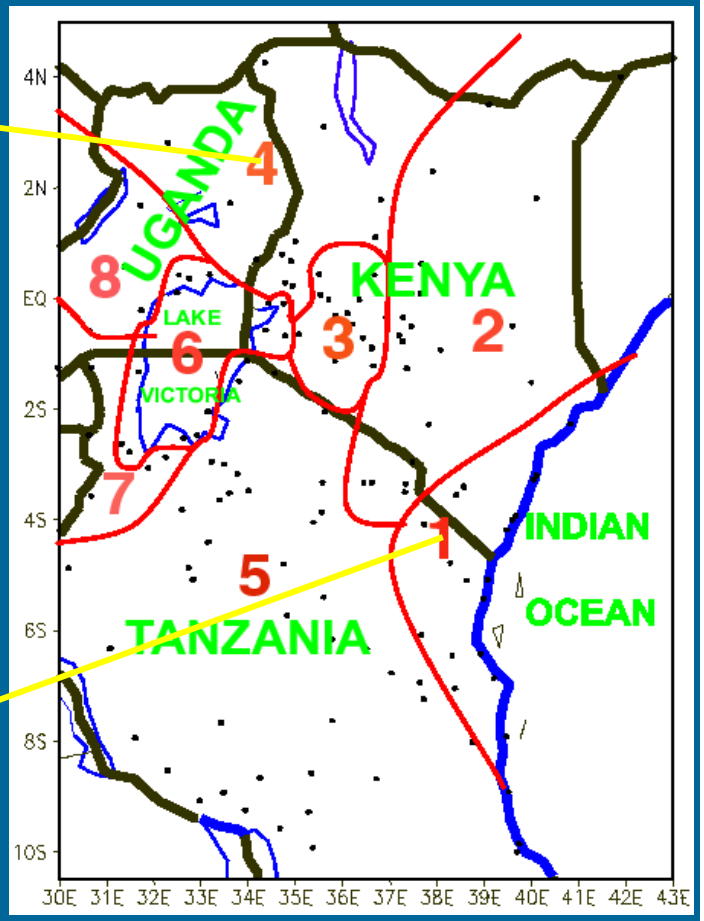

RegCM3 simulated rainfall variability over different homogeneous climate zones

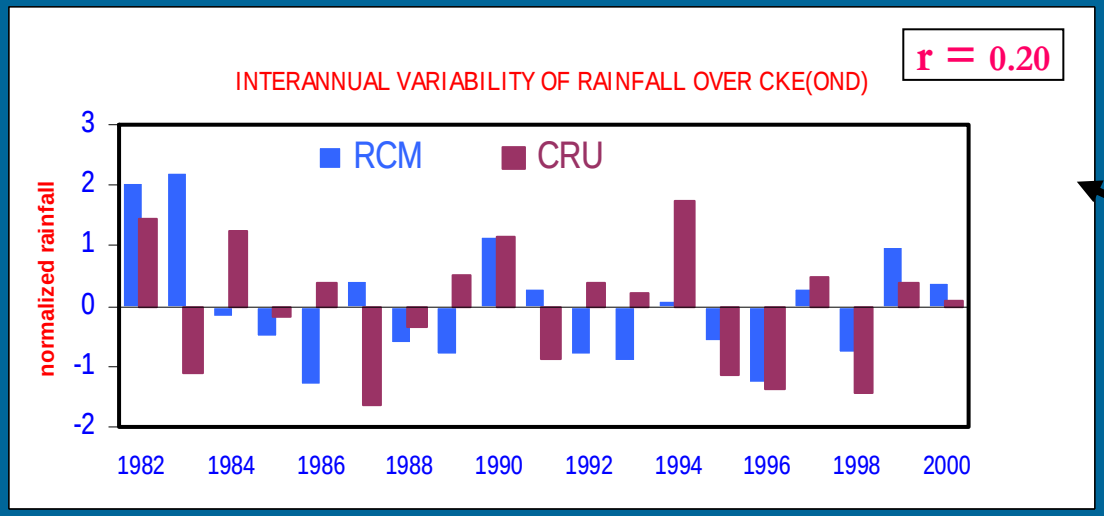

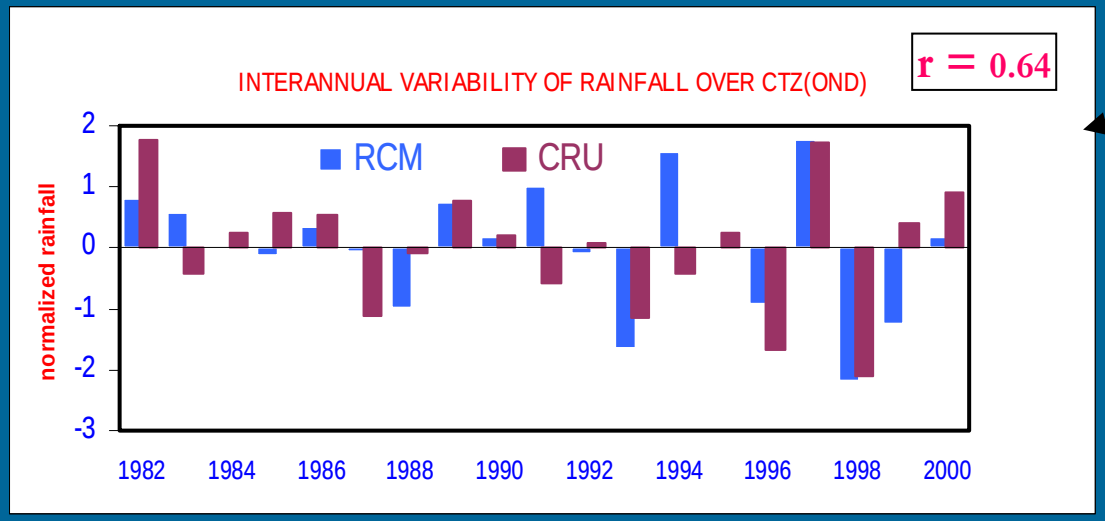

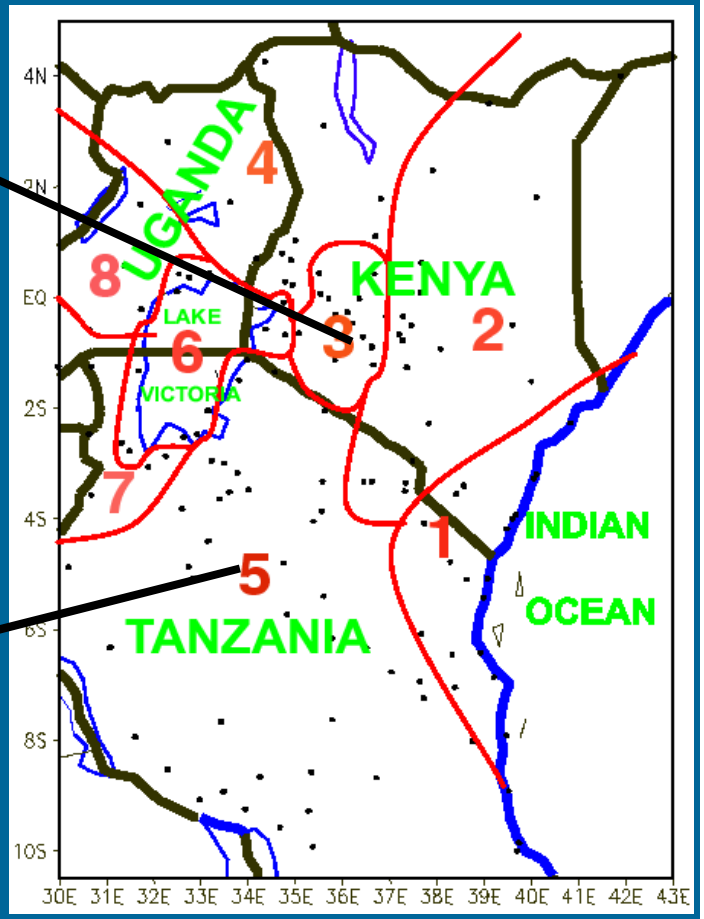

Future Projections ?

Mean surface temperature projections

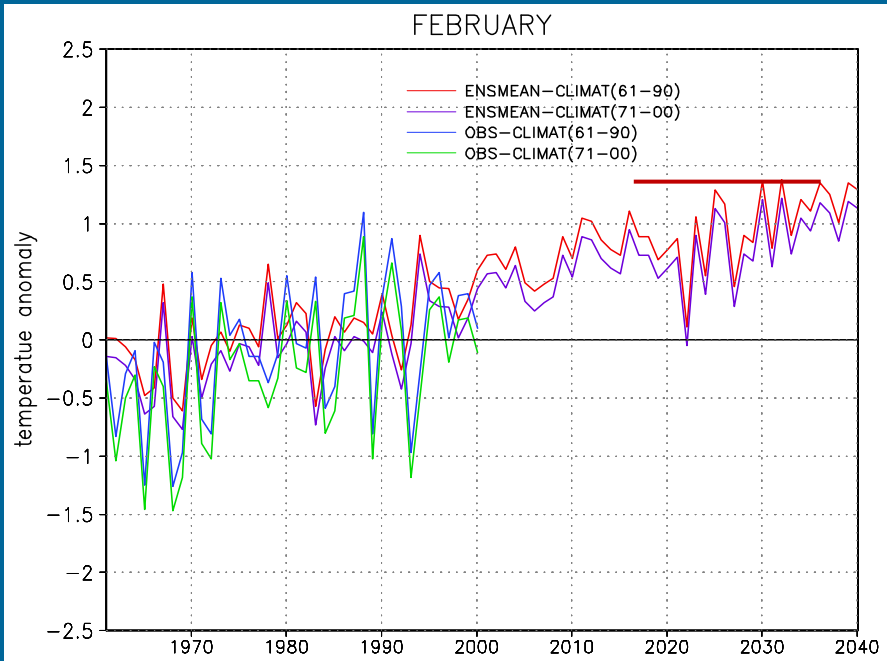

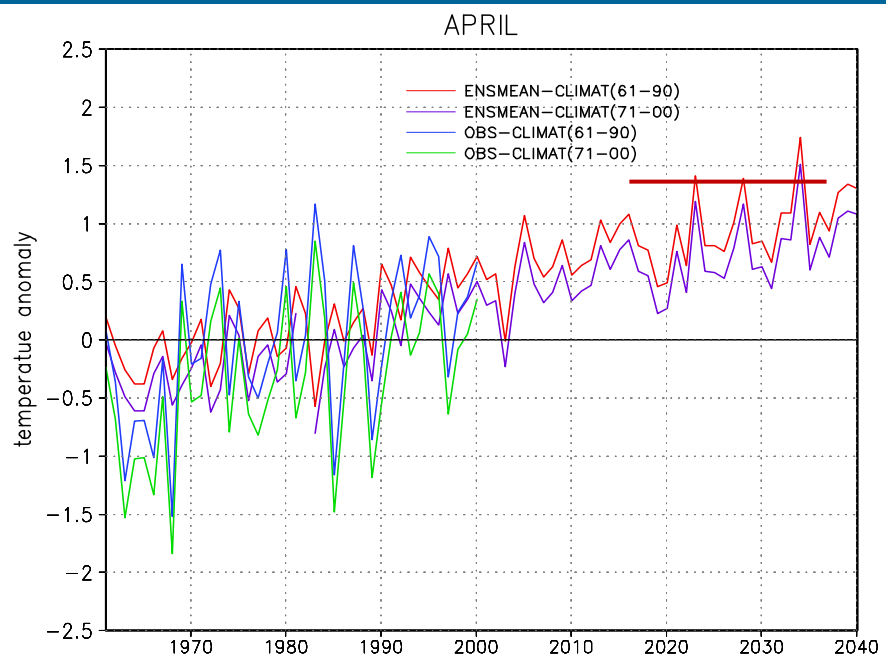

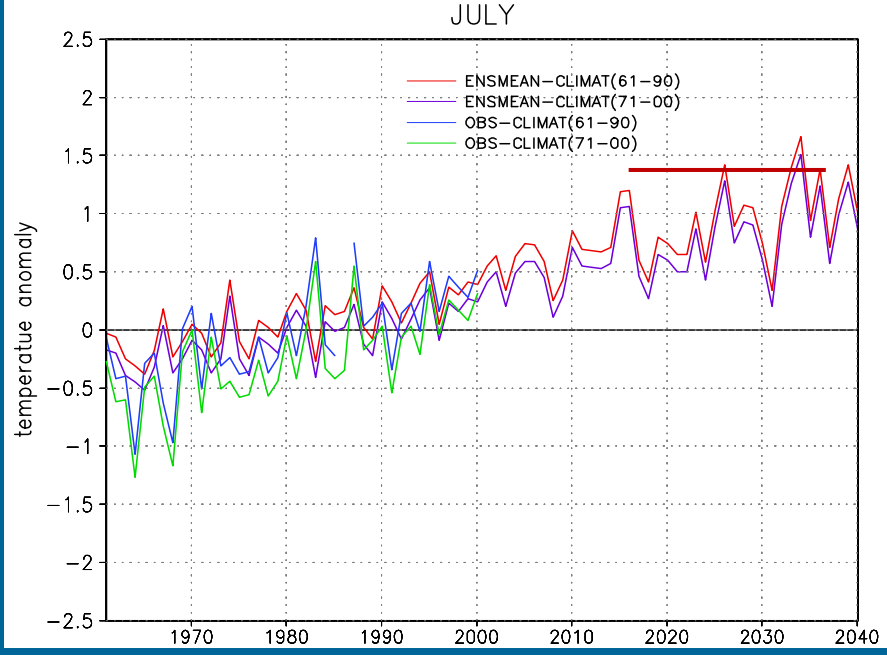

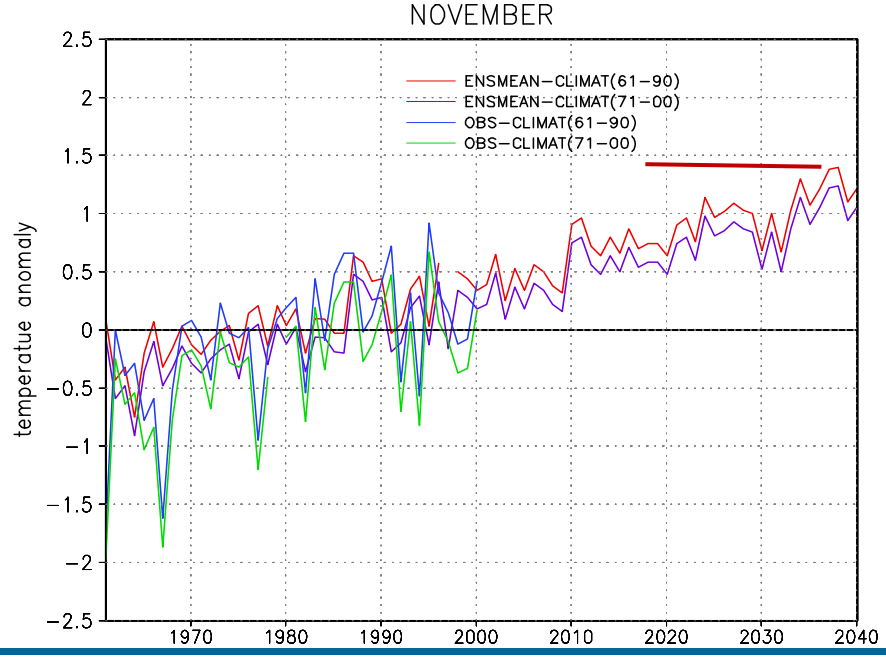

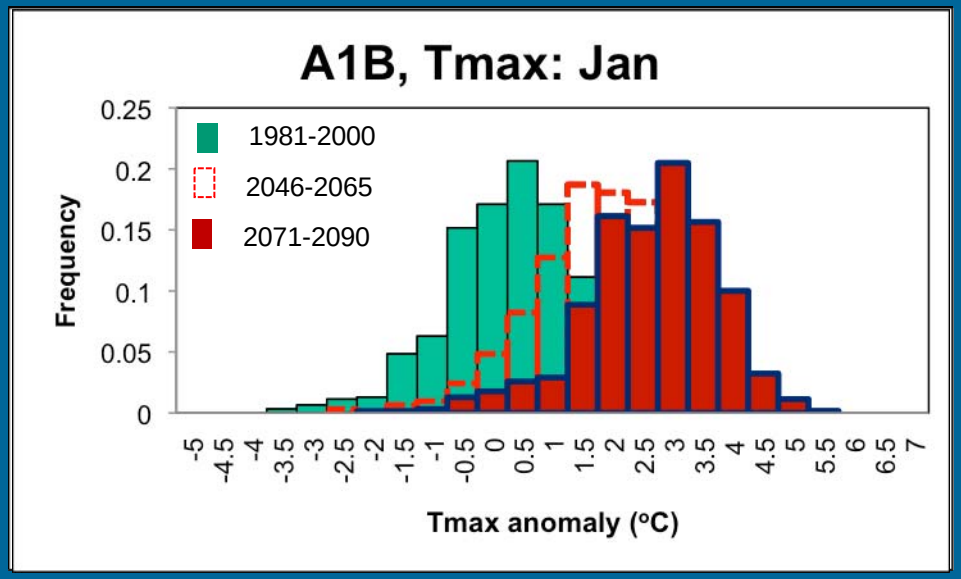
A1B, Tmax: Jan
1981-2000
2046-2065
2071-2090
Frequency
0.25
0.2
0.15
0.1
0.05
0
-5 -4.5 -4 -3.5 -3 -2.5 -2 -1.5 -1 -0.5 0 0.5 1 1.5 2 2.5 3 3.5 4 4.5 5 5.5 6 6.5 7
Tmax anomaly (°C)

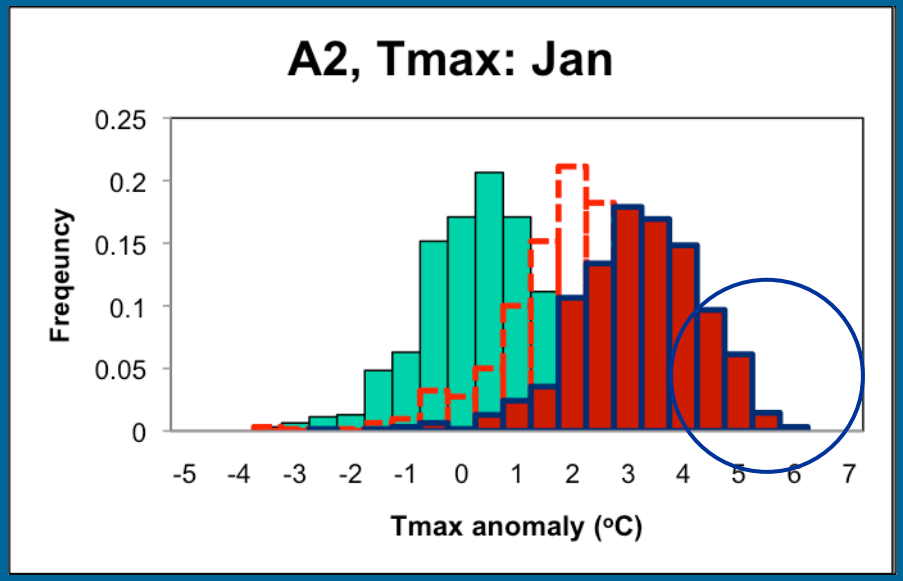
A2, Tmax: Jan
Freqeuncy
0.25
0.2
0.15
0.1
0.05
0
-5 -4 -3 -2 -1 0 1 2 3 4 5 6 7
Tmax anomaly (°C)

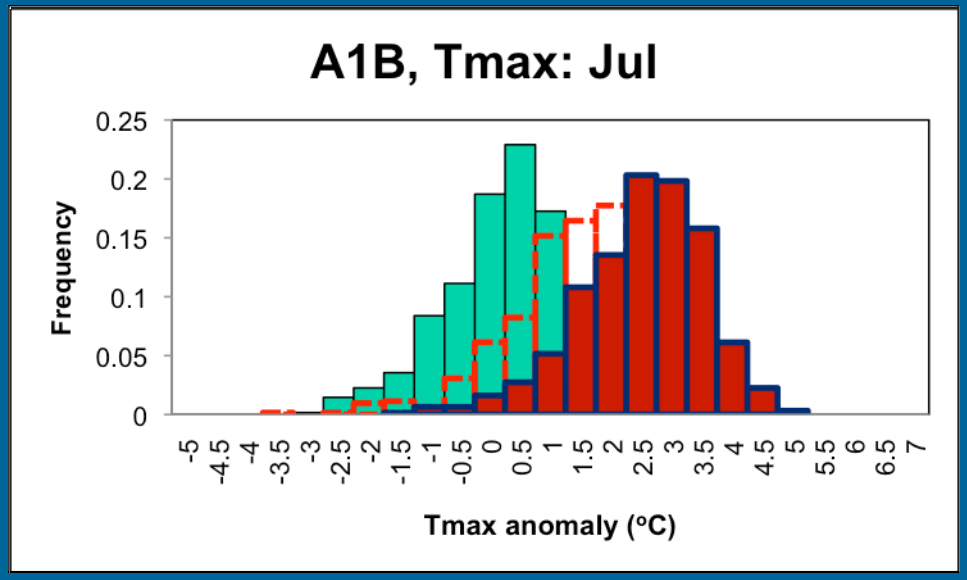
A1B, Tmax: Jul
Frequency
0.25
0.2
0.15
0.1
0.05
0
-5 -4.5 -4 -3.5 -3 -2.5 -2 -1.5 -1 -0.5 0 0.5 1 1.5 2 2.5 3 3.5 4 4.5 5 5.5 6 6.5 7
Tmax anomaly (°C)

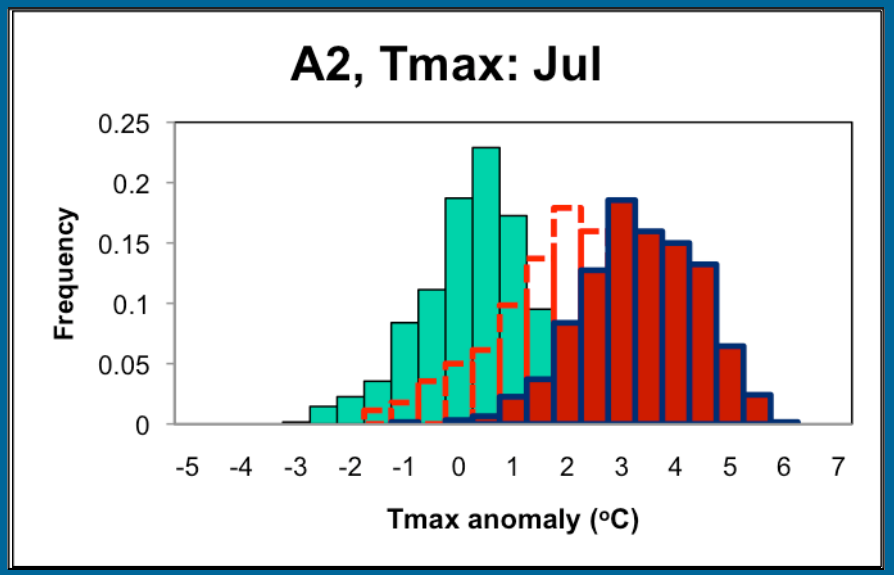
A2, Tmax: Jul
Frequency
0.25
0.2
0.15
0.1
0.05
0
-5 -4 -3 -2 -1 0 1 2 3 4 5 6 7
Tmax anomaly (°C)

Summary & Conclusions

- Delayed transition of flow from SW to NE off the Somalia/East Africa coast during short rains in GCM simulations leading to northward shift in regions of rainfall maximum
- Intra-seasonal to inter-annual variability well reproduced over a number of homogeneous climate sub-regions (in RegCM3 simulations)
- Rainfall variability over central highlands of East Africa (Kenya) and Northeast Kenya poorly reproduced
- Simulated climate using GCM and NCEP lateral boundary forcings are coherent (comparable)
- Both land regions north and south of the equator over the GHA consistently warmed during the period beginning 1990 through 2040. The steepest warming trends during that period occurred in January and July in the A2 scenario simulations by CMIP3 models

Ongoing and Future Work

- Computation of backward trajectories of moisture flux convergence/divergence (Reanalysis and RegCM3) to trace the different moisture sources critical for setting up precipitation anomalies over the Greater Horn of Africa

- Conduct a suite of RegCM3 simulations with imposed (prescribed) SST anomalies over western Indian Ocean

- A suite of regional model simulations with prescribed (satellite-derived) historical land use and cover changes (especially over the tropical-Congo rainforest and parts of GHA region)

- Dynamics of Somali jet in relation to the Indian monsoon and low pressure cell over Sudan and it's relation to rainfall over northern GHA during extreme events

THANK YOU!

DJF 1961-1997 CRU Precipitation difference, velocity potential (10^{-5} m^2/s) and divergent wind (m/s) difference for (a) NCEP at 850 hPa, (b) ERA40 at 850 hPa (c) NCEP at 200 hPa and (d) ERA40 at 200 hPa.

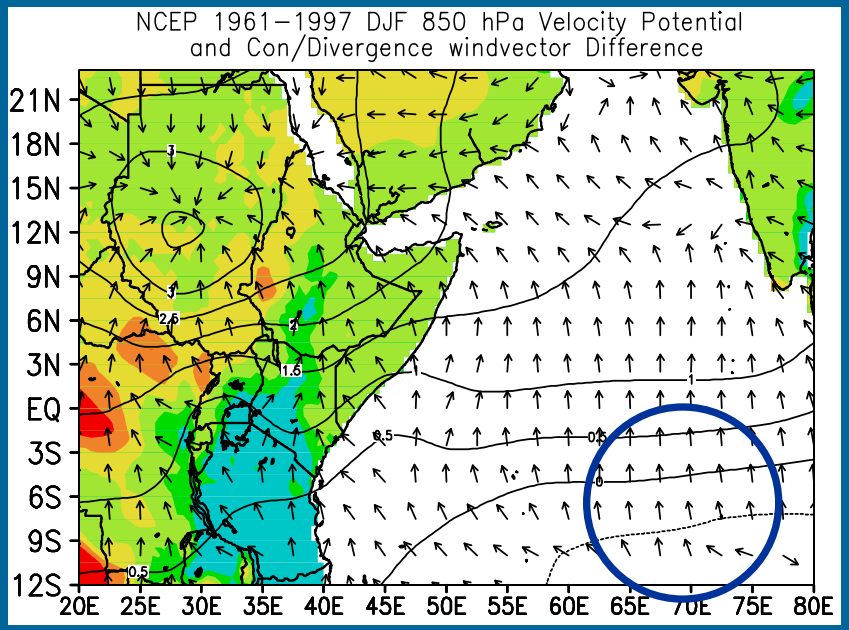

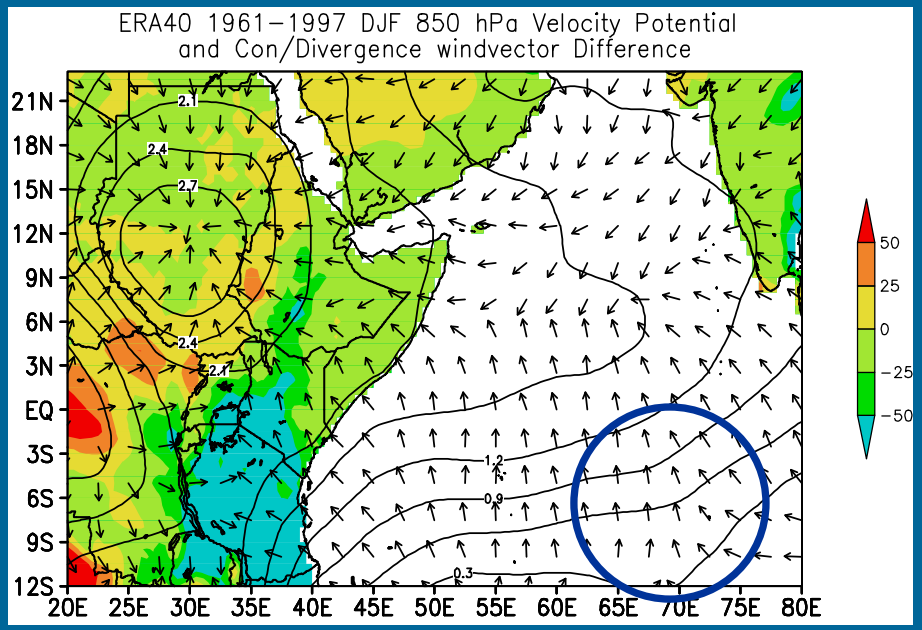

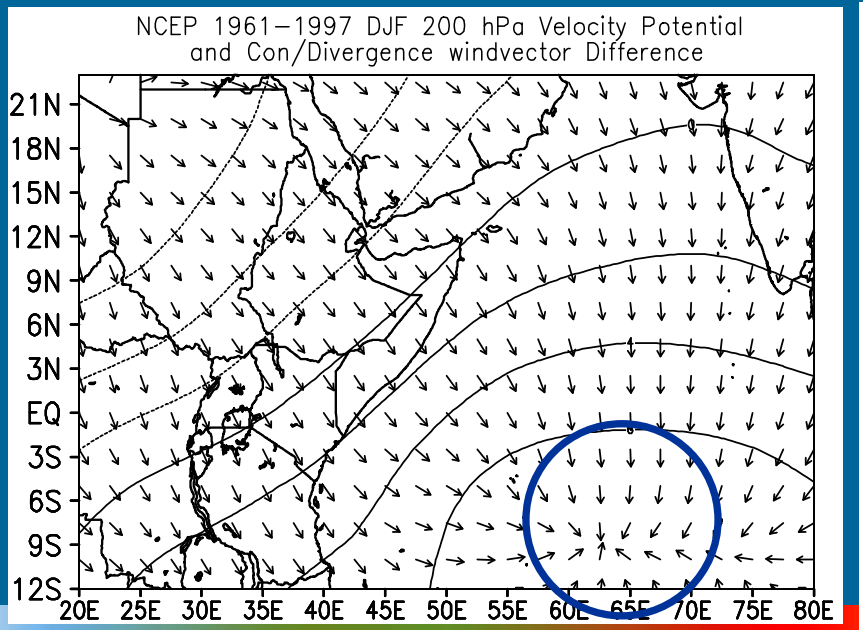

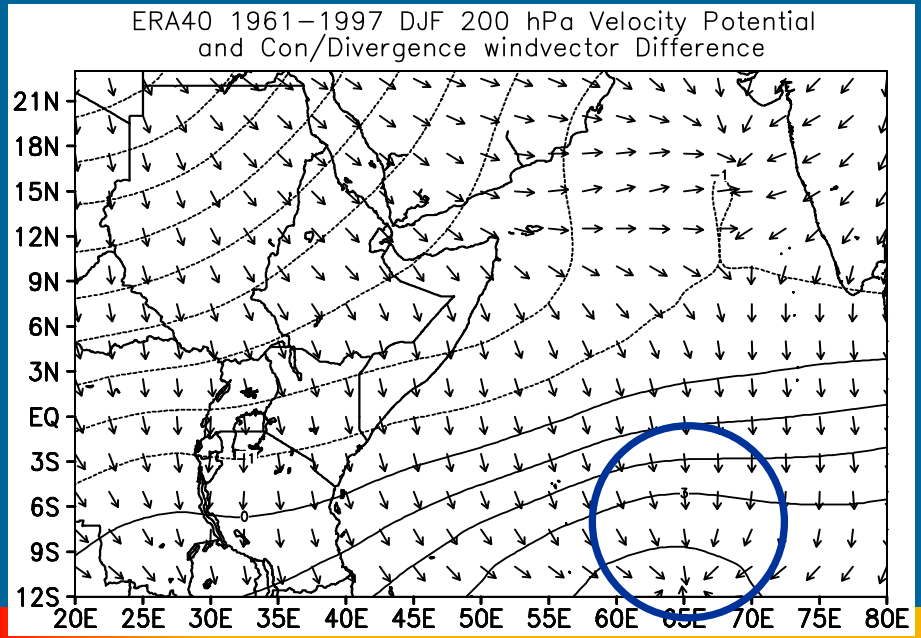

NCEP 1961–1997 DJF 850 hPa Velocity Potential
and Con/Divergence windvector Difference

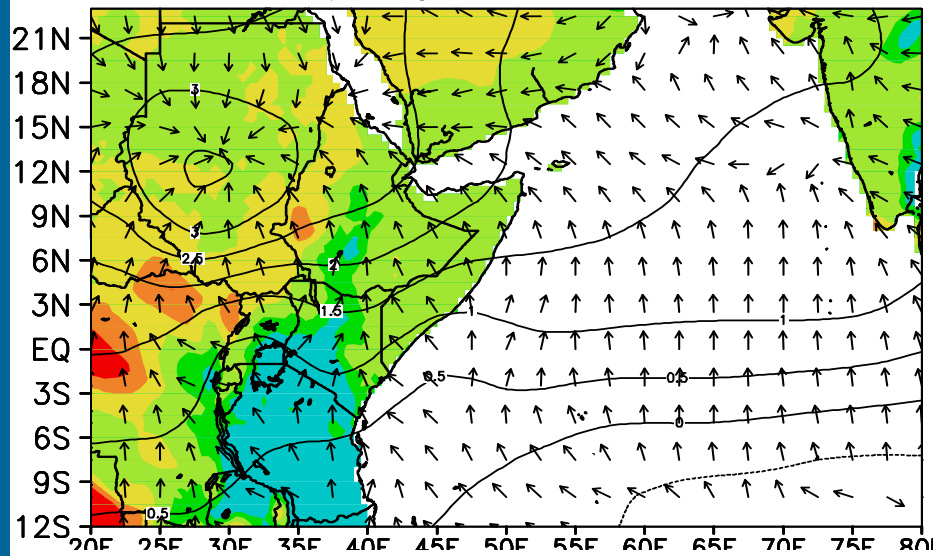

ERA40 1961–1997 DJF 850 hPa Velocity Potential
and Con/Divergence windvector Difference

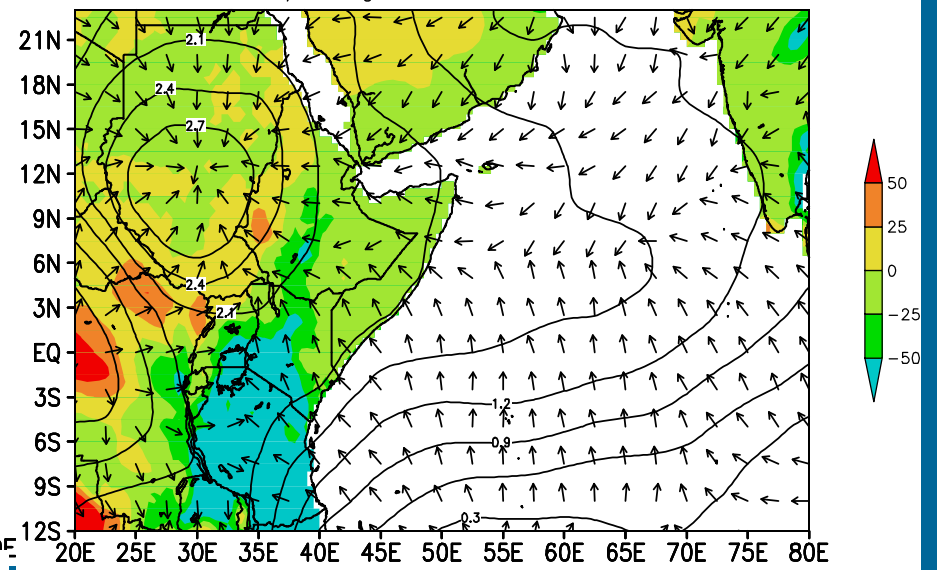

NCEP 1961–1997 DJF 200 hPa Velocity Potential
and Con/Divergence windvector Difference

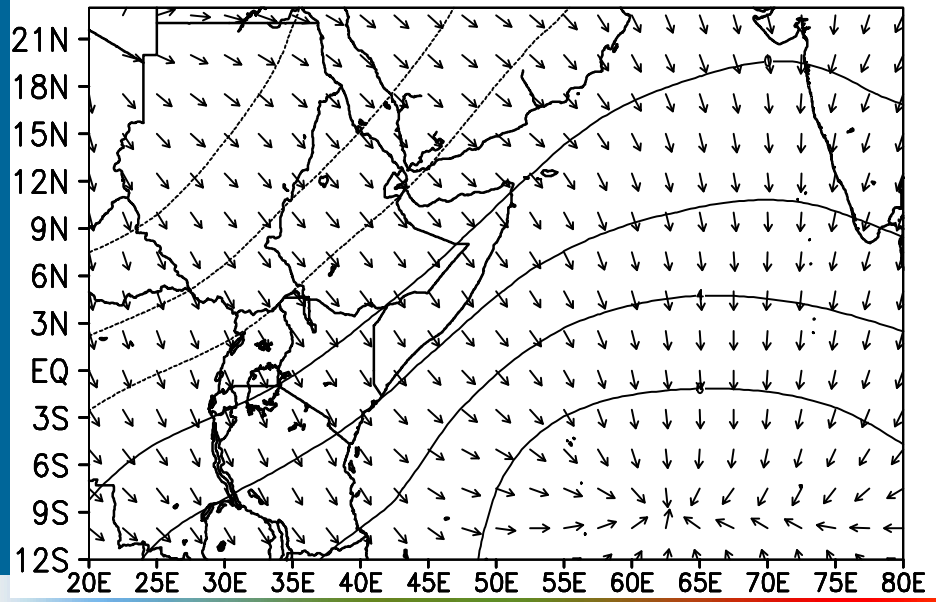

ERA40 1961–1997 DJF 200 hPa Velocity Potential
and Con/Divergence windvector Difference

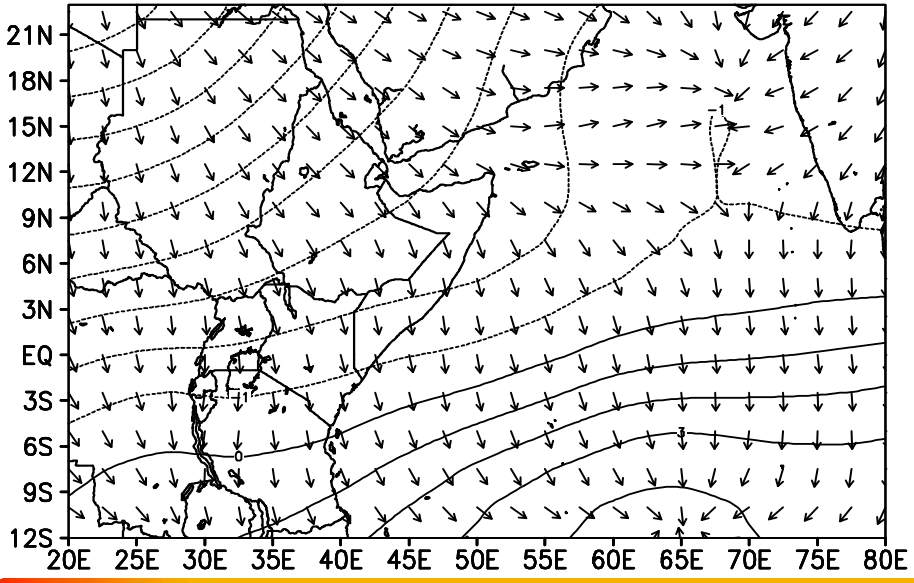

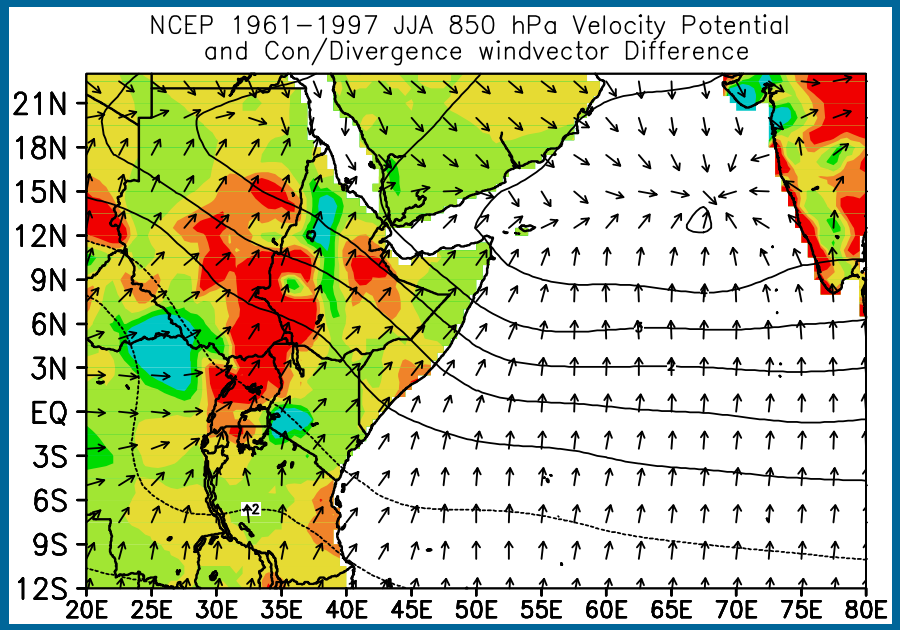
NCEP 1961–1997 JJA 850 hPa Velocity Potential
and Con/Divergence windvector Difference
21N
18N
15N
12N
9N
6N
3N
EQ
3S
6S
9S
12S
20E 25E 30E 35E 40E 45E 50E 55E 60E 65E 70E 75E 80E

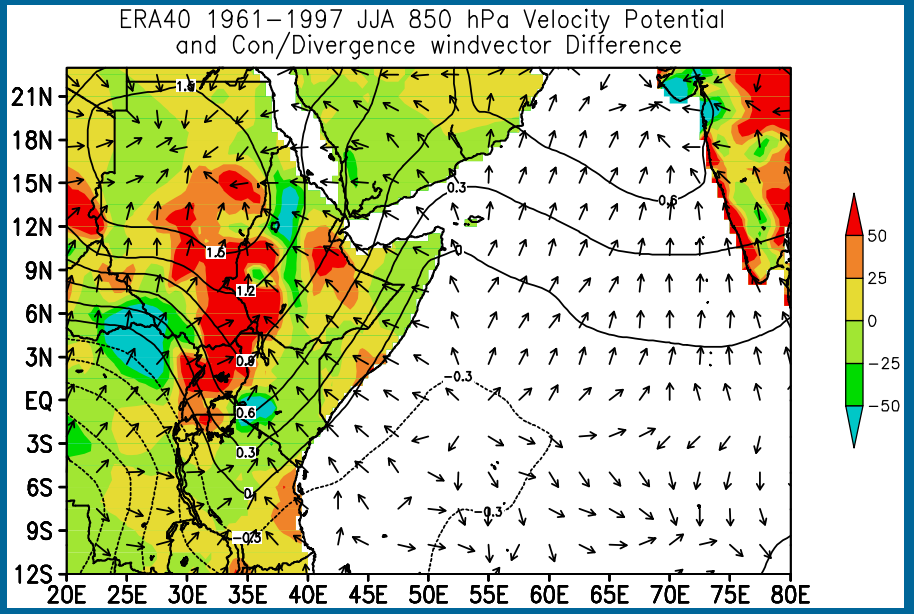
ERA40 1961–1997 JJA 850 hPa Velocity Potential
and Con/Divergence windvector Difference
21N
18N
15N
12N
9N
6N
3N
EQ
3S
6S
9S
12S
20E 25E 30E 35E 40E 45E 50E 55E 60E 65E 70E 75E 80E
50
25
0
−25
−50

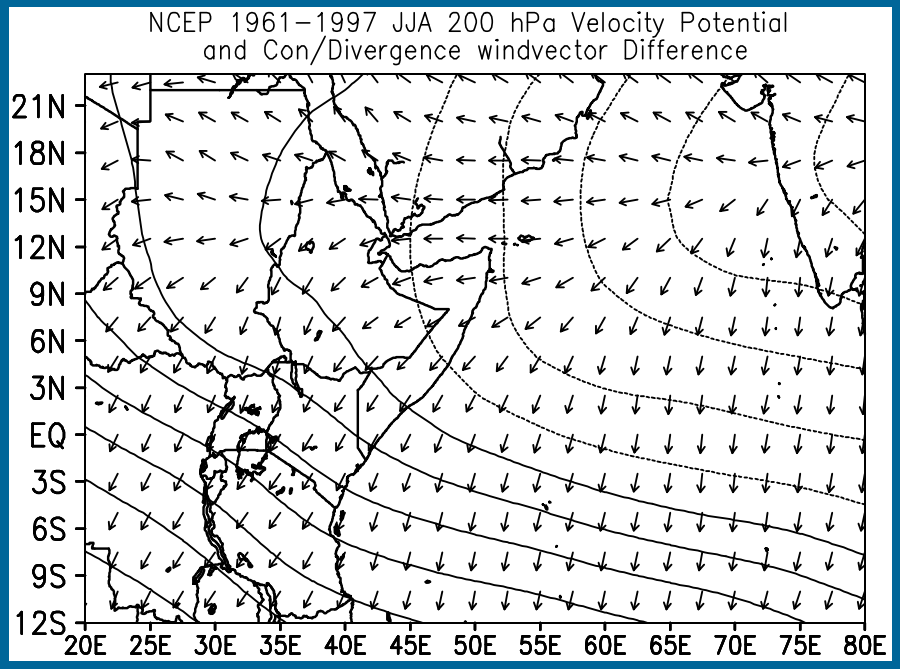
NCEP 1961–1997 JJA 200 hPa Velocity Potential
and Con/Divergence windvector Difference
21N
18N
15N
12N
9N
6N
3N
EQ
3S
6S
9S
12S
20E 25E 30E 35E 40E 45E 50E 55E 60E 65E 70E 75E 80E

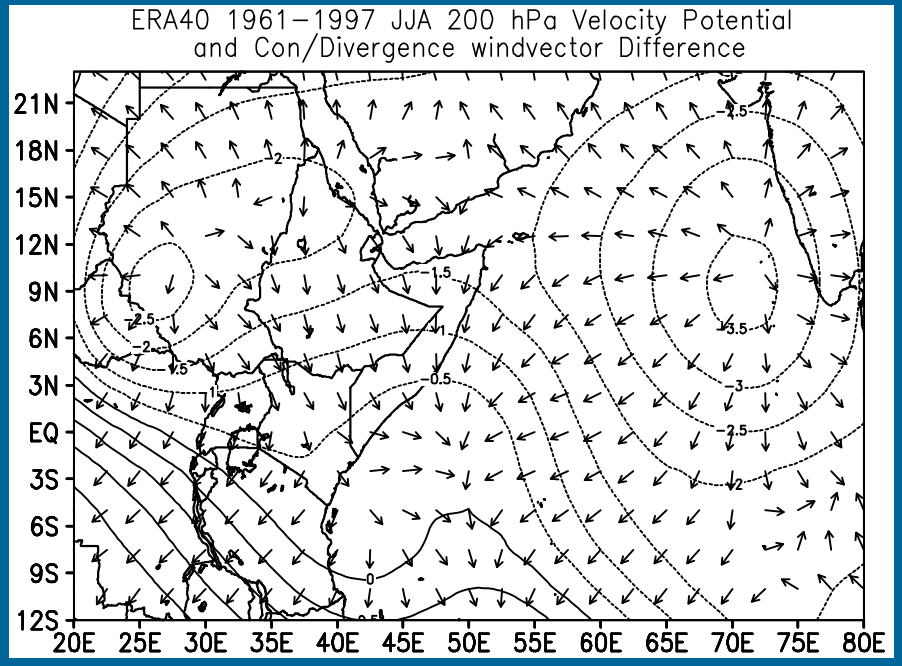
ERA40 1961–1997 JJA 200 hPa Velocity Potential
and Con/Divergence windvector Difference
21N
18N
15N
12N
9N
6N
3N
EQ
3S
6S
9S
12S
20E 25E 30E 35E 40E 45E 50E 55E 60E 65E 70E 75E 80E